myeloid leukemia in Down syndrome. Blood. 2013;121(21):4377-4387.

43) Ohba R, Furuyama K, Yoshida K, Fujiwara T, Fukuhara N, Onishi Y, Manabe A, Ito E, Ozawa K, Kojima S, Ogawa S, Harigae H. Clinical and genetic characteristics of congenital sideroblastic anemia: comparison with myelodysplastic syndrome with ring sideroblast (MDS-RS). Ann Hematol. 2013;92(1):1-9.

44) Nishimura R, Takita J, Sato-Otsubo A, Kato M, Koh K, Hanada R, Tanaka Y, Kato K, Maeda D, Fukayama M, Sanada M, Hayashi Y, Ogawa S. Characterization of genetic lesions in rhabdomyosarcoma using a high-density single nucleotide polymorphism array. Cancer Sci. 2013;104(7):856-864.

45) 17) Ninomiya H, Kato M, Sanada M, Takeuchi K, Inamura K, Motoi N, Nagano H, Nomura K, Sakao Y, Okumura S, Mano H, Ogawa S, Ishikawa Y. Allelotypes of lung adenocarcinomas featuring ALK fusion demonstrate fewer onco- and suppressor gene changes. BMC cancer. 2013;13(1):8.

46) Muto T, Sashida G, Oshima M, Wendt GR, Mochizuki-Kashio M, Nagata Y, Sanada M, Miyagi S, Saraya A, Kamio A, Nagae G, Nakaseko C, Yokote K, Shimoda K, Koseki H, Suzuki Y, Sugano S, Aburatani H, Ogawa S, Iwama A. Concurrent loss of Ezh2 and Tet2 cooperates in the pathogenesis of myelodysplastic disorders. J Exp Med. 2013;210(12):2627-2639.

47) Makishima H, Yoshida K, Nguyen N, Przychodzen B, Sanada M, Okuno Y, Ng KP, Gudmundsson KO, Vishwakarma BA, Jerez A, Gomez-Segui I, Takahashi M, Shiraishi Y, Nagata Y, Guinta K, Mori H, Sekeres MA, Chiba K, Tanaka H, Muramatsu H, Sakaguchi H, Paquette RL, McDevitt MA, Kojima S, Saunthararajah Y, Miyano S, Shih LY, Du Y, Ogawa S, Maciejewski JP. Somatic SETBP1 mutations in myeloid malignancies. Nat Genet. 2013;45(8):942-946.

48) Mae S, Shono A, Shiota F, Yasuno T, Kajiwara M, Gotoda-Nishimura N, Arai S, Sato-Otubo A, Toyoda T, Takahashi K, Nakayama N, Cowan CA, Aoi T, Ogawa S, McMahon AP, Yamanaka S, Osafune K. Monitoring and robust induction of nephrogenic intermediate mesoderm from human pluripotent stem cells. Nat Commun. 2013;4:1367.

49) Lee DH, Amanat S, Goff C, Weiss LM, Said JW, Doan NB, Sato-Otsubo A, Ogawa S, Forscher C, Koeffler HP. Overexpression of miR-26a-2 in human liposarcoma is correlated with poor patient survival. Oncogenesis. 2013;2:e47.

50) Kunishima S, Okuno Y, Yoshida K, Shiraishi Y, Sanada M, Muramatsu H, Chiba K, Tanaka H, Miyazaki K, Sakai M, Ohtake M, Kobayashi R, Iguchi A, Niimi G, Otsu M, Takahashi Y, Miyano S, Saito H, Kojima S, Ogawa S. ACTN1 Mutations Cause Congenital Macrothrombocytopenia. Am J Hum Genet. 2013;92(3):431-438.

51) Kunishima S, Imai T, Kobayashi R, Kato M, Ogawa S, Saito H. Bernard-Soulier syndrome caused by a hemizygous GPIbbeta mutation and 22q11.2 deletion. Pediatr Int. 2013;55(4):434-437.

52) Kon S, Minegishi N, Tanabe K, Watanabe T, Funaki T, Wong WF, Sakamoto D, Higuchi Y, Kiyonari H, Asano K, Iwakura Y, Fukumoto M, Osato M, Sanada M, Ogawa S, Nakamura T, Satake M. Smap1 deficiency perturbs receptor trafficking and

predisposes mice to myelodysplasia. The Journal of clinical investigation. 2013;123(3):1123-1137.

53) Kon A, Shih LY, Minamino M, Sanada M, Shiraishi Y, Nagata Y, Yoshida K, Okuno Y, Bando M, Nakato R, Ishikawa S, Sato-Otsubo A, Nagae G, Nishimoto A, Haferlach C, Nowak D, Sato Y, Alpermann T, Nagasaki M, Shimamura T, Tanaka H, Chiba K, Yamamoto R, Yamaguchi T, Otsu M, Obara N, Sakata-Yanagimoto M, Nakamaki T, Ishiyama K, Nolte F, Hofmann WK, Miyawaki S, Chiba S, Mori H, Nakauchi H, Koeffler HP, Aburatani H, Haferlach T, Shirahige K, Miyano S, Ogawa S. Recurrent mutations in multiple components of the cohesin complex in myeloid neoplasms. Nat Genet. 2013;45(10):1232-1237.

54) Kitamura K, Yoshida K, Shiraishi Y, Chiba K, Tanaka H, Furukawa K, Miyano S, Ogawa S, Kunishima S. Normal neutrophil myosin IIA localization in an immunofluorescence analysis can rule out MYH9 disorders. J Thromb Haemost. 2013;11(11):2071-2073.

55) Kawamata N, Moreilhon C, Saitoh T, Karasawa M, Bernstein BK, Sato-Otsubo A, Ogawa S, Raynaud S, Koeffler HP. Genetic differences between Asian and Caucasian chronic lymphocytic leukemia. International journal of oncology. 2013;43(2):561-565.

56) Kato M, Yasui N, Seki M, Kishimoto H, Sato-Otsubo A, Hasegawa D, Kiyokawa N, Hanada R, Ogawa S, Manabe A, Takita J, Koh K. Aggressive transformation of juvenile myelomonocytic leukemia associated with duplication of oncogenic KRAS due to acquired uniparental disomy. J Pediatr. 2013;162(6):1285-1288, 1288 e1281.

57) Hira A, Yabe H, Yoshida K, Okuno Y, Shiraishi Y, Chiba K, Tanaka H, Miyano S, Nakamura J, Kojima S, Ogawa S, Matsuo K, Takata M, Yabe M. Variant ALDH2 is associated with accelerated progression of bone marrow failure in Japanese Fanconi anemia patients. Blood. 2013.

58) Haferlach T, Nagata Y, Grossmann V, Okuno Y, Bacher U, Nagae G, Schnittger S, Sanada M, Kon A, Alpermann T, Yoshida K, Roller A, Nadarajah N, Shiraishi Y, Shiozawa Y, Chiba K, Tanaka H, Koeffler HP, Klein HU, Dugas M, Aburatani H, Kohlmann A, Miyano S, Haferlach C, Kern W, Ogawa S. Landscape of Genetic Lesions in 944 Patients with Myelodysplastic Syndromes. Leukemia. 2013.

59) Gomez-Segui I, Makishima H, Jerez A, Yoshida K, Przychodzen B, Miyano S, Shiraishi Y, Husseinzadeh HD, Guinta K, Clemente M, Hosono N, McDevitt MA, Moliterno AR, Sekeres MA, Ogawa S, Maciejewski JP. Novel recurrent mutations in the RAS-like GTP-binding gene RIT1 in myeloid malignancies. Leukemia. 2013;27(9):1943-1946.

60) Damm F, Chesnais V, Nagata Y, Yoshida K, Scourzic L, Okuno Y, Itzykson R, Sanada M, Shiraishi Y, Gelsi-Boyer V, Renneville A, Miyano S, Mori H, Shih LY, Park S, Dreyfus F, Guerci-Bresler A, Solary E, Rose C, Cheze S, Prebet T, Vey N, Legentil M, Duffourd Y, de Botton S, Preudhomme C, Birnbaum D, Bernard OA, Ogawa S, Fontenay M, Kosmider O. BCOR and BCORL1 mutations in myelodysplastic syndromes and related disorders. Blood. 2013;122(18):3169-3177.

61) Asanuma S, Yamagishi M, Kawanami K, Nakano K, Sato-Otsubo A, Muto S, Sanada M, Yamochi T, Kobayashi S, Utsunomiya A, Iwanaga M, Yamaguchi K, Uchimaru K, Ogawa S, Watanabe T. Adult T-cell leukemia cells are characterized by abnormalities of Helios expression that promote T cell growth. Cancer Sci. 2013;104(8):1097-1106.

62) Sakata-Yanagimoto M, Enami T, Yoshida K, Shiraishi Y, Ishii R, Miyake Y, Muto H, Tsuyama N, Sato-Otsubo A, Okuno Y, Sakata S, Kamada Y, Nakamoto-Matsubara R, Tran NB, Izutsu K, Sato Y, Ohta Y, Furuta J, Shimizu S, Komeno T, Sato Y, Ito T, Noguchi M, Noguchi E, Sanada M, Chiba K, Tanaka H, Suzukawa K, Nanmoku T, Hasegawa Y, Nureki O, Miyano S, Nakamura N, Takeuchi K, Ogawa S, Chiba S. Somatic RHOA mutation in angioimmunoblastic T cell lymphoma. Nat Genet. 2014.

63) Lin TL, Nagata Y, Kao HW, Sanada M, Okuno Y, Huang CF, Liang DC, Kuo MC, Lai CL, Lee EH, Shih YS, Tanaka H, Shiraishi Y, Chiba K, Lin TH, Wu JH, Miyano S, Ogawa S, Shih LY. Clonal leukemic evolution in myelodysplastic syndromes with TET2 and IDH1/2 mutations. Haematologica. 2014;99(1):28-36.

64) Hosono N, Makishima H, Jerez A, Yoshida K, Przychodzen B, McMahon S, Shiraishi Y, Chiba K, Tanaka H, Miyano S, Sanada M, Gomez-Segui I, Verma AK, McDevitt MA, Sekeres MA, Ogawa S, Maciejewski JP. Recurrent genetic defects on chromosome 7q in myeloid neoplasms. Leukemia. 2014.

65) Becker H, Yoshida K, Blagitko-Dorfs N,Claus R, Pantic M,Abdelkarim M, Niemöller C, Greil C, Hackanson B, Shiraishi Y, Chiba K, Tanaka H, Miyano S, Döhner K, Schnittger S, Henneke P, Niemeyer C, Flotho C, Pfeifer D, Ogawa S, Lübbert M Tracing the development of acute myeloid leukemia in CBL-syndrome Blood 2014.

2. 学会発表

海外

1) Kenichi Yoshida, Tsutomu Toki, Myoung-ja Park, Yusuke Okuno, Yuichi Shiraishi, Masashi Sanada, Ayana Kon, Yasunobu Nagata, Aiko Sato-Otsubo, Yusuke Sato, RuNan Wang, Kiminori Terui, Rika Kanezaki, Norio Shiba, Kenichi Chiba, Hiroko Tanaka, Asahito Hama, Hideki Muramatsu, Daisuke Hasegawa, Kazuhiro Nakamura, Hirokazu Kanegane, Keiko Tsukamoto, Souichi Adachi, Kiyoshi Kawakami, Seiji Kojima, Shai Izraeli, Satoru Miyano, Yasuhide Hayashi, Etsuro Ito and Seishi Ogawa. Genetic basis of myeloid leukemogenesis in Down syndrome. The 18th Congress of European Hematology Association (EHA) (Oral, Best abstract) 2013/6/15 Stockholm (Sweden)

2) Kenichi Yoshida, Tsutomu Toki, Myoung-ja Park, Yusuke Okuno, Yuichi Shiraishi, Masashi Sanada, Ayana Kon, Yasunobu Nagata, Aiko Sato-Otsubo, Yusuke Sato, RuNan Wang, Kiminori Terui, Rika Kanezaki, Norio Shiba, Kenichi Chiba, Hiroko Tanaka, Asahito Hama, Daisuke Hasegawa, Kazuhiro Nakamura, Hirokazu Kanegane, Keiko Tsukamoto, Souichi Adachi, Satoru Miyano, Seiji Kojima, Shai Izraeli, Yasuhide Hayashi, Etsuro Ito and Seishi Ogawa. Genetic Basis of Myeloid Proliferation Related to Down Syndrome, 2012 American Society of Hematology

(ASH) Annual Meeting and Exposition (Oral, ASH Outstanding Abstract Achievement Award) 2012/12/10 Atlanta (U.S.A.)

3) Hideki Muramatsu, Yusuke Okuno, Hirotoshi Sakaguchi, Kenichi Yoshida, Yuichi Shiraishi, Masashi Sanada, Kenichi Chiba, Hiroko Tanaka, Hideki Makishima, Xinan Wang, Yinyan Xu, Sayoko Doisaki, Asahito Hama, Koji Nakanishi, Yoshiyuki Takahashi, Nao Yoshida, Jaroslaw P. Maciejewski, Satoru Miyano, Seishi Ogawa, Seiji Kojima. Whole Exome Analysis Reveals Spectrum of Gene Mutations in Juvenile Myelomonocytic Leukemia. 54th ASH Annual Meeting and Exposition, 2012.
4) Etsuro Ito, Kenichi Yoshida, Yusuke Okuno, Aiko Sato-Otsubo, Tsutomu Toki, Satoru Miyano, Yuichi Shiraishi, Kenichi Chiba, Kiminori Terui, RuNan Wang, Tomohiko Sato, Yuji Iribe, Shouichi Ohga, Madoka Kuramitsu, Isao Hamaguchi, Akira Ohara, Kazuko Kudo, Isamu Kamimaki, Junichi Hara, Kanji Sugita, Kousaku Matsubara, Kenichi Koike, Akira Ishiguro, Yoshifumi Kawano, Hitoshi Kanno, Seiji Kojima, Seishi Ogawa. Identification of Two New DBA Genes, RPS27 and RPL27, by Whole-Exome Sequencing in Diamond-Blackfan Anemia Patients. 54th ASH Annual Meeting and Exposition, 2012.
5) Kenichi Yoshida, Tsutomu Toki, Myoung-ja Park, Yusuke Okuno, Yuichi Shiraishi, Masashi Sanada, Ayana Kon, Yasunobu Nagata, Aiko Sato-Otsubo, Yusuke Sato, RuNan Wang, Kiminori Terui, Rika Kanezaki, Norio Shiba, Kenichi Chiba, Hiroko Tanaka, Asahito Hama, Daisuke Hasegawa, Kazuhiro Nakamura, Hirokazu Kanegane, Keiko Tsukamoto, Souichi Adachi, Satoru Miyano, Seiji Kojima, Shai Izraeli, Yasuhide Hayashi, Etsuro Ito, Seishi Ogawa. Genetic Basis of Myeloid Proliferation Related to Down Syndrome. 54th ASH Annual Meeting and Exposition, 2012.
6) Seishi Ogawa.Genetic analysis of myeloid neoplasms in childhood. Cambridge Research Institute Annual International Symposium. 2012/11/2 Cambridge (UK)
7) Seishi Ogawa, Genetic analysis of Down Syndrome-related myeloid neoplasms. 日仏がんワークショップ 2013/11/22, Toulouse (France)

国内

1) 吉田健一、小川誠司、國島伸治　血小板異常症　第 116 回日本小児科学会学術集会 2013/4/19 広島
2) 吉田健一、小川誠司 次世代シーケンサーを用いた先天性造血器疾患の全ゲノム・全エクソン解析 第 54 回日本小児血液・がん学会学術集会 2012/12/2 横浜
3) Kenichi Yoshida, Tsutomu Toki, Myoung-ja Park, Yusuke Okuno, Yuichi Shiraishi, Masashi Sanada, Ayana Kon, Yasunobu Nagata, Aiko Sato-Otsubo, Yusuke Sato, RuNan Wang, Kiminori Terui, Rika Kanezaki, Norio Shiba, Kenichi Chiba, Hiroko Tanaka, Asahito Hama, Hideki Muramatsu, Daisuke Hasegawa, Kazuhiro Nakamura, Hirokazu Kanegane, Keiko Tsukamoto, Souichi Adachi, Kiyoshi Kawakami, Seiji Kojima, Shai Izraeli, Satoru Miyano, Yasuhide Hayashi, Etsuro Ito and Seishi Ogawa. Genetic basis of myeloid leukemogenesis in Down syndrome. 第75回日本血液学会学術集会 2013/10/11 札幌
4) 吉田健一、土岐力、朴明子、永田安伸、王汝南、白石友一、真田昌、昆彩菜、佐藤亜衣子、

長崎正朗、宮野悟、金兼弘和、川上清、加藤剛二、小島勢二、林泰秀、伊藤悦朗、小川誠司 ダウン症候群に合併した一過性骨髄増殖症（TAM）および急性巨核芽球性白血病（AMKL）の全エクソンシーケンス 第53回日本小児血液・がん学会学術集会

5) 小川誠司, 加藤元博, 林泰秀. TAMにおける遺伝学的基盤探索. 第114回日本小児科学会学術集会 2011/4

G. 知的財産権の出願・登録状況

なし

Ⅲ．研究成果の刊行に関する一覧

発表者氏名	論文タイトル名	発表誌名	巻名	ページ	出版年
Yoshida K, Sanada M, Shiraishi Y, Nowak D, Nagata Y, Yamamoto R, Sato Y, Sato-Otsubo A, Kon A, Nagasaki M, Chalkidis G, Suzuki Y, Shiosaka M, Kawahata R, Yamaguchi T, Otsu M, Obara N, Sakata-Yanagimoto M, Ishiyama K, Mori H, Nolte F, Hofmann WK, Miyawaki S, Sugano S, Haferlach C, Koeffler HP, Shih LY, Haferlach T, Chiba S, Nakauchi H, Miyano S, Ogawa S.	Frequent pathway mutations of splicing machinery in myelodysplasia.	Nature	478	64-9	2011
Kunishima S, Kashiwagi H, Otsu M, Takayama N, Eto K, Onodera M, Miyajima Y, Takamatsu Y, Suzumiya J, Matsubara K, Tomiyama Y, Saito H.	Heterozygous *ITGA2B* R995W mutation inducing constitutive activation of the αIIbβ3 receptor affects proplatelet formation and causes congenital macrothrombocytopenia.	Blood	117	5479-84	2011
Murata Y, Yasumi T, Shirakawa R, Izawa K, Sakai H, Abe J, Tanaka N, Kawai T, Oshima K, Saito M, Nishikomori R, Ohara O, Ishii E, Nakahata T, Horiuchi H, Heike T.	Rapid diagnosis of familial hemophagocytic lymphohistiocytosis type 3 (FHL3) by flow cytometric detection of intraplatelet Munc13-4 protein.	Blood	118	1225-30	2011
Rosado IV, Langevin F, Crossan GP, Takata M, Patel KJ.	Formaldehyde catabolism is essential in cells deficient for the Fanconi anemia DNA-repair pathway.	Nat Struct Mol Biol	18 (12)	1432-4	2011
Doisaki S, Muramatsu H, Shimada A, Takahashi Y, Mori-Ezaki M, Sato M, Kawaguchi H, Kinoshita A, Sotomatsu M, Hayashi Y, Furukawa-Hibi Y, Yamada K, Hoshino H, Kiyoi H, Yoshida N, Sakaguchi H, Narita A, Wang X, Ismael O, Xu Y, Nishio N, Tanaka M, Hama A, Koike K, Kojima S.	Somatic mosaicism for oncogenic NRAS mutations in juvenile myelomonocytic leukemia.	Blood	120 (7)	1485-8	2012
Sato K, Ishiai M, Toda K, Furukoshi S, Osakabe A, Tachiwana H, Takizawa Y, Kagawa W, Kitao H, Dohmae N, Obuse C, Kimura H, Takata M, Kurumizaka H.	Histone chaperone activity of Fanconi anemia proteins, FANCD2 and FANCI, is required for DNA crosslink repair.	EMBO J.	21	3524-36	2012
Kuramitsu M, Sato-Otsubo A, Morio T, Takagi M, Toki T, Terui K, RuNan Wang, Kanno H, Ohga S, Ohara A, Kojima S, Kitoh T, Goi K, Kudo K, Matsubayashi T, Mizue N, Ozeki M, Masumi A, Momose H, Takizawa K, Mizukami T, Yamaguchi K, Ogawa S, Ito E, Hamaguchi I.	Extensive gene deletions in Japanese patients with Diamond–Blackfan anemia.	Blood	119 (10)	2376-84	2012
Yokoyama T, Toki T, Aoki Y, Park MJ, Kanno Y, Tanaka T, Yamazaki Y. Ito E, Hayashi Y, Nakamura T.	Identification of *TRIB1* R107L gain-of-function mutation in human acute megakaryocytic leukemia.	Blood	119 (11)	2608-11	2012
Honda F, Kano H, Kanegane H, Nonoyama S, Kim ES, Lee SK, Takagi M, Mizutani S, Morio T.	The kinase Btk negatively regulates the production of reactive oxygen species and stimulation-induced apoptosis in human neutrophils	Nat Immunol	13	369-78	2012

Gruber TA, Larson Gedman A, Zhang J, Koss CS, Marada S, Ta HQ, Chen SC, Su X, Ogden SK, Dang J, Wu G, Gupta V, Andersson AK, Pounds S, Shi L, Easton J, Barbato MI, Mulder HL, Manne J, Wang J, Rusch M, Ranade S, Ganti R, Parker M, Ma J, Radtke I, Ding L, Cazzaniga G, Biondi A, Kornblau SM, Ravandi F, Kantarjian H, Nimer SD, Döhner K, Döhner H, Ley TJ, Ballerini P, Shurtleff S, Tomizawa D, Adachi S, Hayashi Y, Tawa A, Shih LY, Liang DC, Rubnitz JE, Pui CH, Mardis ER, Wilson RK, Downing JR.	An Inv(16)(p13.3q24.3)-Encoded CBFA2T3- GLIS2 Fusion Protein Defines an Aggressive Subtype of Pediatric Acute Megakaryoblastic Leukemia.	Cancer Cell	22	683-97	2012
Miyawaki Y, Suzuki A, Fujita J, Maki A, Okuyama E, Murata M, Takagi A, Murate T, Kunishima S, Sakai M, Okamoto K, Matsushita T, Naoe T, Saito H, Kojima T	Thrombosis from a prothrombin mutation conveying antithrombin-resistance	New Engl J Med	366	2390-6	2012
Hiramoto T, Ebihara Y, Mizoguchi Y, Nakamura K, Yamaguchi K, Ueno K, Mochizuki S, Yamamoto S, Nagasaki M, Furukawa Y, Tani K, Nakauchi H. Kobayashi M, Tsuji K.	Wnt3a stimulates maturation of impaired neutrophils developed from severe congenital neutropenia-derived pluipotent stem cells with heterozygous *ELANE* mutation.	Proc Natl Acad Sci USA	110 (8)	3023-8	2013
Sakaguchi H, Nakanishi K, Kojima S.	Inherited bone marrow failure syndromes in 2012.	Int J Hematol.	97(1)	20-9	2013
Makishima H, Yoshida K, Nguyen N, Przychodzen B, Sanada M, Okuno Y, Ng KP, Gudmundsson KO, Vishwakarma BA, Jerez A, Gomez-Segui I, Takahashi M, Shiraishi Y, Nagata Y, Guinta K, Mori H, Sekeres MA, Chiba K, Tanaka H, Muramatsu H, Sakaguchi H, Paquette RL, McDevitt MA, Kojima S, Sauntharajah Y, Miyano S, Shih LY, Du Y, Ogawa S, Maciejewski JP.	Somatic SETBP1 mutations in myeloid malignancies.	Nat Genet.	45(8)	942-6	2013
Sakaguchi H, Okuno Y, Muramatsu H, Yoshida K, Shiraishi Y, Takahashi M, Kon A, Sanada M, Chiba K, Tanaka H, Makishima H, Wang X, Xu Y, Doisaki S, Hama A, Nakanishi K, Takahashi Y, Yoshida N, Maciejewski JP, Miyano S, Ogawa S, Kojima S.	Exome sequencing identifies secondary mutations of SETBP1 and JAK3 in juvenile myelomonocytic leukemia.	Nat Genet.	45(8)	937-41	2013
Takahashi Y, Muramatsu H, Sakata N, Hyakuna N, Hamamoto K, Kobayashi R, Ito E, Yagasaki H, Ohara A, Kikuchi A, Morimoto A, Yabe H, Kudo K, Watanabe K, Ohga S, Kojima S, Japan Childhood Aplastic Anemia Study G.	Rabbit antithymocyte globulin and cyclosporine as first-line therapy for children with acquired aplastic anemia.	Blood	121 (5)	862-3	2013
Hira A, Yabe H, Yoshida K, Okuno Y, Shiraishi Y, Chiba K, Tanaka H, Miyano S, Nakamura J, Kojima S, Ogawa S, Matsuo K, Takata M and Yabe M.	Variant ALDH2 is associated with accelerated progression of bone marrow failure in Japanese Fanconi anemia patients.	Blood	122 (18)	3206-9	2013

Saida S, Watanabe K, Sato-Otsubo A, Terui K, Yoshida K, Okuno Y, Toki T, Wang R, Shiraishi Y, Miyano S, Kato I, Morishima T, Fujino H, Umeda K, Hiramatsu H, Adachi S, Ito E, Ogawa S, Ito M, Nakahata T, Heike T.	Clonal selection in xenografted TAM recapitulates the evolutionary process of myeloid leukemia in Down syndrome.	Blood	121 (21)	4377-87	2013
Yoshida K, Toki T, Okuno Y, Kanezaki R, Shiraishi Y, Sanada M, Park M, Terui K, Kon A, Nagata Y, Sato-Otsubo A, Sato Y, Wang R, Shiba N, Chiba K, Tanaka H, Hama A, Muramatsu H, Hasegawa D, Nakamura K, Kanegane H, Tsukamoto K, Adachi S, Kawakami K, Kato K, Nishimura R, Izraeli S, Hayashi Y, Miyano S, Kojima S, Ito E, Seishi Ogawa S.	The Landscape of gene mutations in Down syndrome-related myeloid disorders.	Nat Genet.	45 (11)	1293-9	2013
Toki T, Kanezaki R, Kobayashi E, Kaneko H, Suzuki M, Wang R, Terui K, Kanegane H, Maeda M, Endo M, Mizuochi T, Adachi S, Hayashi Y, Yamamoto M, Shimizu R, Ito E.	Naturally occurring oncogenic GATA1 mutants with internal deletions in transient abnormal myelopoiesis in Down syndrome.	Blood	121 (16)	3181-4	2013
Hirata S, Takayama N, Jono-Ohnishi R, Endo H, Nakamura S, Dohda T, Nishi M, Hamazaki Y, Ishii E, Kaneko S, Otsu M, Nakauchi H, Kunishima S, Eto K.	Congenital amegakaryocytic thrombocytopenia iPS cells exhibit defective MPL-mediated signaling.	J Clin Invest.	123 (9)	3802-14	2013
Noris P, Favier R, Alessi MC, Geddis AE, Kunishima S, Heller PG, Giordano P, Niederhoffer K, Bussel JB, Podda M, Vianelli N, Kensseboom R, Pecci A, Gnam C, Marconi C, Auvrignon A, Cohen W, Yu JC, Iguchi A, Imahiyerobo AM, Boehlen F, Ghalloussi D, De Rocco D, Magini P, Civaschi E, Biino G, Seri M, Savoia A, Balduini CL.	*ANKRD26*-related thrombocytopenia and myeloid malignancies.	Blood	122 (11)	1987-9	2013
Kon A, Shih LY, Minamino M, Sanada M, Shiraishi Y, Nagata Y, Yoshida K, Okuno Y, Bando M, Nakato R, Ishikawa S, Sato-Otsubo A, Nagae G, Nishimoto A, Haferlach C, Nowak D, Sato Y, Alpermann T, Nagasaki M, Shimamura T, Tanaka H, Chiba K, Yamamoto R, Yamaguchi T, Otsu M, Obara N, Sakata-Yanagimoto M, Nakamaki T, Ishiyama K, Nolte F, Hofmann WK, Miyawaki S, Chiba S, Mori H, Nakauchi H, Koeffler HP, Aburatani H, Haferlach T, Shirahige K, Miyano S, Ogawa S.	Recurrent mutations in multiple components of the cohesin complex in myeloid neoplasms.	Nat Genet.	45 (10)	1232-7	2013
Sato Y, Yoshizato T, Shiraishi Y, Maekawa S, Okuno Y, Kamura T, Shimamura T, Sato-Otsubo A, Nagae G, Suzuki H, Nagata Y, Yoshida K, Kon A, Suzuki Y, Chiba K, Tanaka H, Niida A, Fujimoto A, Tsunoda T, Morikawa T, Maeda D, Kume H, Sugano S, Fukayama M, Aburatani H, Sanada M, Miyano S, Homma Y, Ogawa S.	Integrated molecular analysis of clear-cell renal cell carcinoma.	Nat Genet.	45(8)	860-7	2013

Deenick EK, Avery DT, Chan A, Berglund LJ, Ives ML, Moens L, Stoddard JL, Bustamante J, Boisson-Dupuis S, Tsumura M, Kobayashi M, Arkwright PD, Averbuch D, Engelhard D, Roesler J, Peake J, Wong M, Adelstein S, Choo S, Smart JM, French MA, Fulcher DA, Cook MC, Picard C, Durandy A, Klein C, Holland SM, Uzel G, Casanova JL, Ma CS, Tangye SG.	Naive and memory human B cells have distinct requirements for STAT3 activation to differentiate into antibody-secreting plasma cells.	J Exp Med.	210 (12)	2739-56	2013
Kaneko K, Furuyama K, Fujiwara T, Kobayashi R, Ishida H, Harigae H, Shibahara S.	Identification of the novel erythroid-Specific enhancer for ALAS2 gene and its loss-of-function mutation associated with congenital sideroblastic anemia.	Haematologica	99(2)	252-61	2014
Sakata-Yanagimoto M, Enami T, Yoshida K, Shiraishi Y, Ishii R, Miyake Y, Muto H, Tsuyama N, Sato-Otsubo A, Okuno Y, Sakata S, Kamada Y, Nakamoto-Matsubara R, Tran NB, Izutsu K, Sato Y, Ohta Y, Furuta J, Shimizu S, Komeno T, Sato Y, Ito T, Noguchi M, Noguchi E, Sanada M, Chiba K, Tanaka H, Suzukawa K, Nanmoku T, Hasegawa Y, Nureki O, Miyano S, Nakamura N, Takeuchi K, Ogawa S, Chiba S.	Somatic RHOA mutation in angioimmunoblastic T cell lymphoma.	Nat Genet.	46(2)	171-5	2014

Ⅳ．研究成果の刊行物・別刷り

doi:10.1038/nature10496

Frequent pathway mutations of splicing machinery in myelodysplasia

Kenichi Yoshida[1]*, Masashi Sanada[1]*, Yuichi Shiraishi[2]*, Daniel Nowak[3]*, Yasunobu Nagata[1]*, Ryo Yamamoto[4], Yusuke Sato[1], Aiko Sato-Otsubo[1], Ayana Kon[1], Masao Nagasaki[5], George Chalkidis[6], Yutaka Suzuki[7], Masashi Shiosaka[1], Ryoichiro Kawahata[1], Tomoyuki Yamaguchi[8], Makoto Otsu[4], Naoshi Obara[9], Mamiko Sakata-Yanagimoto[9], Ken Ishiyama[10], Hiraku Mori[11], Florian Nolte[3], Wolf-Karsten Hofmann[3], Shuichi Miyawaki[10], Sumio Sugano[7], Claudia Haferlach[12], H. Phillip Koeffler[13,14], Lee-Yung Shih[15], Torsten Haferlach[12], Shigeru Chiba[9], Hiromitsu Nakauchi[4,8], Satoru Miyano[2,6] & Seishi Ogawa[1]

Myelodysplastic syndromes and related disorders (myelodysplasia) are a heterogeneous group of myeloid neoplasms showing deregulated blood cell production with evidence of myeloid dysplasia and a predisposition to acute myeloid leukaemia, whose pathogenesis is only incompletely understood. Here we report whole-exome sequencing of 29 myelodysplasia specimens, which unexpectedly revealed novel pathway mutations involving multiple components of the RNA splicing machinery, including *U2AF35*, *ZRSR2*, *SRSF2* and *SF3B1*. In a large series analysis, these splicing pathway mutations were frequent (~45 to ~85%) in, and highly specific to, myeloid neoplasms showing features of myelodysplasia. Conspicuously, most of the mutations, which occurred in a mutually exclusive manner, affected genes involved in the 3′-splice site recognition during pre-mRNA processing, inducing abnormal RNA splicing and compromised haematopoiesis. Our results provide the first evidence indicating that genetic alterations of the major splicing components could be involved in human pathogenesis, also implicating a novel therapeutic possibility for myelodysplasia.

Myelodysplastic syndromes (MDS) and related disorders (myelodysplasia) comprise a group of myeloid neoplasms characterized by deregulated, dysplastic blood cell production and a predisposition to acute myeloid leukaemia (AML)[1]. Although the prevalence of MDS has not been determined precisely, more than 10,000 people are estimated to develop myelodysplasia annually in the United States[2]. Their indolent clinical course before leukaemic transformation and ineffective haematopoiesis with evidence of myeloid dysplasia indicate a pathogenesis distinct from that involved in *de novo* AML. Currently, a number of gene mutations and cytogenetic changes have been implicated in the pathogenesis of MDS, including mutations of *RAS*, *TP53* and *RUNX1*, and more recently *ASXL1*, *c-CBL*, *DNMT3A*, *IDH1/2*, *TET2* and *EZH2* (ref. 3). Nevertheless, mutations of this set of genes do not fully explain the pathogenesis of MDS because they are also commonly found in other myeloid malignancies and roughly 20% of MDS cases have no known genetic changes (ref. 4 and unpublished data). In particular, the genetic alterations responsible for the dysplastic phenotypes and ineffective haematopoiesis of myelodysplasia are poorly understood. Meanwhile, the recent development of massively parallel sequencing technologies has provided an expanded opportunity to discover genetic changes across the entire genomes or protein-coding sequences in human cancers at a single-nucleotide level[5–10], which could be successfully applied to the genetic analysis of myelodysplasia to obtain a better understanding of its pathogenesis.

Overview of genetic alterations

In this study, we performed whole-exome sequencing of paired tumour/control DNA from 29 patients with myelodysplasia (Supplementary Table 1). Although incapable of detecting non-coding mutations and gene rearrangements, the whole-exome approach is a well-established strategy for obtaining comprehensive registries of protein-coding mutations at low cost and high performance. With a mean coverage of 133.8, 80.4% of the target sequences were analysed at more than ×20 depth on average (Supplementary Fig. 1). All the candidates for somatic mutations ($N = 497$) generated through our data analysis pipeline were subjected to validation using Sanger sequencing (Supplementary Methods I and Supplementary Fig. 2). Finally, 268 non-synonymous somatic mutations were confirmed with an overall true positive rate of 53.9% (Supplementary Fig. 3), including 206 missense, 25 nonsense, and 10 splice site mutations, and 27 frameshift-causing insertions/deletions (indels) (Supplementary Fig. 4). The mutation rate of 9.2 (0–21) per sample was significantly lower than that in solid tumours (16.2–302)[7,11,12] and multiple myeloma (32.4)[6], but was comparable to that in AML (7.3–13)[13–15] and chronic lymphocytic leukaemia (11.5)[16]. Combined with the genomic copy number profile obtained by single nucleotide polymorphism (SNP) array karyotyping, this array of somatic mutations provided a landscape of myelodysplasia genomes (Supplementary Fig. 5)[17,18].

[1]Cancer Genomics Project, Graduate School of Medicine, The University of Tokyo, 7-3-1 Hongo, Bunkyo-ku, Tokyo 113-8655, Japan. [2]Laboratory of DNA Information Analysis, Human Genome Center, Institute of Medical Science, The University of Tokyo, 4-6-1 Shirokanedai, Minato-ku, Tokyo 108-8639, Japan. [3]Department of Hematology and Oncology, Medical Faculty Manheim of the University of Heidelberg, 1-3 Theodor-Kutzer-Ufer, Mannheim 68167, Germany. [4]Division of Stem Cell Therapy, Center for Stem Cell Biology and Regenerative Medicine, Institute of Medical Science, The University of Tokyo, 4-6-1 Shirokanedai, Minato-ku, Tokyo 108-8639, Japan. [5]Laboratory of Functional Genomics, Human Genome Center, Institute of Medical Science, The University of Tokyo, 4-6-1 Shirokanedai, Minato-ku, Tokyo 108-8639, Japan. [6]Laboratory of Sequence Data Analysis, Human Genome Center, Institute of Medical Science, The University of Tokyo, 4-6-1 Shirokanedai, Minato-ku, Tokyo 108-8639, Japan. [7]Division of Systems Biomedical Technology, Institute of Medical Science, The University of Tokyo, 4-6-1 Shirokanedai, Minato-ku, Tokyo 108-8639, Japan. [8]Nakauchi Stem Cell and Organ Regeneration Project, Exploratory Research for Advanced Technology, Japan Science and Technology Agency, 4-6-1 Shirokanedai, Minato-ku, Tokyo 108-8639, Japan. [9]Department of Hematology, Institute of Clinical Medicine, University of Tsukuba, 1-1-1 Tennodai, Tsukuba-shi, Ibaraki, 305-8571, Japan. [10]Division of Hematology, Tokyo Metropolitan Ohtsuka Hospital, 2-8-1 Minami-Ohtsuka, Toshima-ku, Tokyo 170-0005, Japan. [11]Division of Hematology, Internal Medicine, Showa University Fujigaoka Hospital, 1-30 Fujigaoka, Aoba-ku, Yokohama, Kanagawa 227-8501, Japan. [12]Munich Leukemia Laboratory, Max-Lebsche-Platz 31, Munich 81377, Germany. [13]Hematology/Oncology, Cedars-Sinai Medical Center, 8700 Beverly Blvd, Los Angeles, California 90048, USA. [14]National University of Singapore, Cancer Science Institute of Singapore, 28 Medical Drive, Singapore 117456, Singapore. [15]Division of Hematology-Oncology, Department of Internal Medicine, Chang Gung Memorial Hospital, Chang Gung University, 199 Tung Hwa North Rd, Taipei 105, Taiwan.
*These authors contributed equally to this work.

Novel gene targets in myelodysplasia

The list of the somatic mutations (Supplementary Table 2) included most of the known gene targets in myelodysplasia with similar mutation frequencies to those previously reported, indicating an acceptable sensitivity of the current study. The mutations of the known gene targets, however, accounted for only 12.3% of all detected mutations ($N = 33$), and the remaining 235 mutations involved previously unreported genes. Among these, recurrently mutated genes in multiple cases are candidate targets of particular interest, for which high mutation rates are expected in general populations. In fact, 8 of the 12 recurrently mutated genes were among the well-described gene targets in myelodysplasia (Supplementary Table 3). However, what immediately drew our attention were the recurrent mutations involving *U2AF35* (also known as *U2AF1*), *ZRSR2* and *SRSF2* (SC35), because they belong to the common pathway known as RNA splicing. Including an additional three genes mutated in single cases (*SF3A1*, *SF3B1* and *PRPF40B*), six components of the splicing machinery were mutated in 16 out of the 29 cases (55.2%) in a mutually exclusive manner (Fig. 1, Supplementary Fig. 6 and Supplementary Table 2).

Frequent mutations in splicing machinery

RNA splicing is accomplished by a well-ordered recruitment, rearrangement and/or disengagement of a set of small nuclear ribonucleoprotein (snRNP) complexes (U1, U2, and either U4/5/6 or U11/12), as well as many other protein components onto the pre-mRNAs. Notably, the mutated components of the spliceosome were all engaged in the initial steps of RNA splicing, except for PRPF40B, whose functions in RNA splicing are poorly defined. Making physical interactions with SF1 and a serine/arginine-rich (SR) protein, such as SRSF1 or SRSF2, the U2 auxiliary factor (U2AF) that consists of the U2AF65 (U2AF2)–U2AF35 heterodimer, is involved in the recognition of the 3′ splice site (3′SS) and its nearby polypyrimidine tract, which is thought to be required for the subsequent recruitment of the U2 snRNP, containing SF3A1 as well as SF3B1, to establish the splicing A complex (Fig. 1)[19]. ZRSR2 (or Urp), is another essential component of the splicing machinery. Showing a close structural similarity to U2AF35, ZRSR2 physically interacts with U2AF65, as well as SRSF1 and SRSF2, with a distinct function from its homologue, U2AF35 (ref. 20).

To confirm and extend the initial findings in the whole-exome sequencing, we studied mutations of the above six genes together with three additional spliceosome-related genes, including *U2AF65*, *SF1* and *SRSF1*, in a large series of myeloid neoplasms ($N = 582$) using a high-throughput mutation screen of pooled DNA followed by confirmation/identification of candidate mutations (refs 21 and 22 and Supplementary Methods II).

In total, 219 mutations were identified in 209 out of the 582 specimens of myeloid neoplasms through validating 313 provisional positive events in the pooled DNA screen (Supplementary Tables 4 and 5). The mutations among four genes, *U2AF35* ($N = 37$), *SRSF2* ($N = 56$), *ZRSR2* ($N = 23$) and *SF3B1* ($N = 79$), explained most of the mutations with much lower mutational rates for *SF3A1* ($N = 8$), *PRPF40B* ($N = 7$), *U2AF65* ($N = 4$) and *SF1* ($N = 5$) (Fig. 2). Mutations of the splicing machinery were highly specific to diseases showing myelodysplastic features, including MDS either with (84.9%) or without (43.9%) increased ring sideroblasts, chronic myelomonocytic leukaemia (CMML) (54.5%), and therapy-related AML or AML with myelodysplasia-related changes (25.8%), but were rare in *de novo* AML (6.6%) and myeloproliferative neoplasms (MPN) (9.4%) (Fig. 3a). The mutually exclusive pattern of the mutations in these splicing pathway genes was confirmed in this large case series, suggesting a common impact of these mutations on RNA splicing and the pathogenesis of myelodysplasia (Fig. 3b). The frequencies of mutations showed significant differences across disease types. Surprisingly, *SF3B1* mutations were found in the majority of the cases with MDS characterized by increased ring sideroblasts, that is, refractory anaemia with ring sideroblasts (RARS) (19/23 or 82.6%) and refractory cytopenia with multilineage dysplasia with ≥ 15% ring sideroblasts (RCMD-RS) (38/50 or 76%) with much lower mutation frequencies in other myeloid neoplasms. RARS and RCMD-RS account

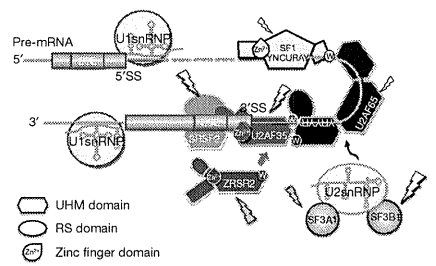

Figure 1 | Components of the splicing E/A complex mutated in myelodysplasia. RNA splicing is initiated by the recruitment of U1 snRNP to the 5′SS. SF1 and the larger subunit of the U2 auxiliary factor (U2AF), U2AF65, bind the branch point sequence (BPS) and its downstream polypyrimidine tract, respectively. The smaller subunit of U2AF (U2AF35) binds to the AG dinucleotide of the 3′SS, interacting with both U2AF65 and a SR protein, such as SRSF2, through its UHM and RS domain, comprising the earliest splicing complex (E complex). ZRSR2 also interacts with U2AF and SR proteins to perform essential functions in RNA splicing. After the recognition of the 3′SS, U2 snRNP, together with SF3A1 and SF3B1, is recruited to the 3′SS to generate the splicing complex A. The mutated components in myelodysplasia are indicated by arrows.

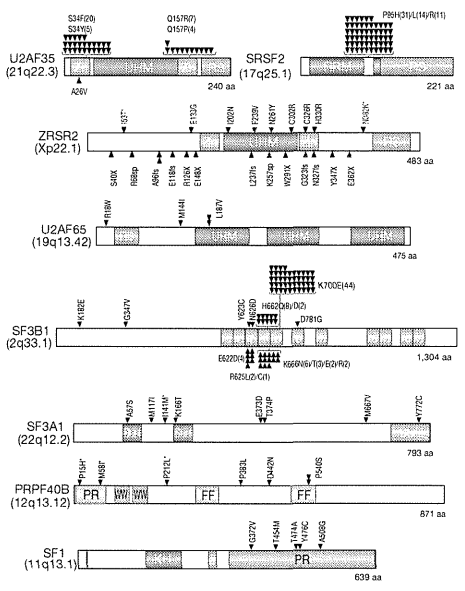

Figure 2 | Mutations of multiple components of the splicing machinery. Each mutation in the eight spliceosome components is shown with an arrowhead. Confirmed somatic mutations are discriminated by red arrows. Known domain structures are shown in coloured boxes as indicated. Mutations predicted as SNPs by MutationTaster (http://www.mutationtaster.org/) are indicated by asterisks. The number of each mutation is indicated in parenthesis. ZRSR2 mutations in females are shown in blue.

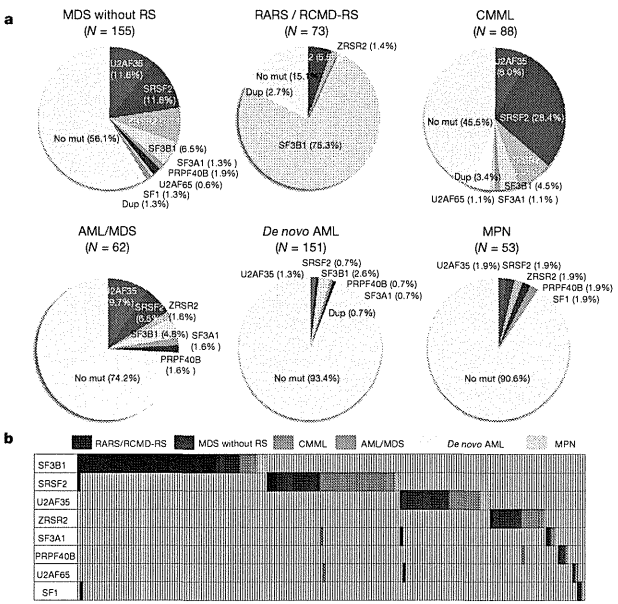

Figure 3 | Frequencies and distribution of spliceosome pathway gene mutations in myeloid neoplasms. **a**, Frequencies of spliceosome pathway mutations among 582 cases with various myeloid neoplasms. **b**, Distribution of mutations in eight spliceosome genes, where diagnosis of each sample is shown by indicated colours.

for 4.3% and 12.9% of MDS cases, respectively, where deregulated iron metabolism has been implicated in the development of refractory anaemia[23]. With such high mutation frequencies and specificity, the *SF3B1* mutations were thought to be almost pathognomonic to these MDS subtypes characterized by increased ring sideroblasts, and strongly implicated in the pathogenesis of MDS in these categories. Less conspicuously but significantly, *SRSF2* mutations were more frequent in CMML cases (Fig. 3 and Supplementary Table 4). Thus, although commonly involving the E/A splicing complexes, different mutations may still have different impacts on cell functions, contributing to the determination of discrete disease phenotypes. For example, studies have demonstrated that *SRSF2* was also involved in the regulation of DNA stability and that depletion of SRSF2 can lead to genomic instability[24]. Of interest in this context, regardless of disease subtypes, samples with *SRSF2* mutations were shown to have significantly more mutations of other genes compared with *U2AF35* mutations ($P = 0.001$, multiple regression analysis) (Supplementary Table 6 and Supplementary Fig. 7).

Notably, with a rare exception of A26V in a single case, the mutations of U2AF35 exclusively involved two highly conserved amino acid positions (S34 or Q157) within the amino- and the carboxyl-terminal zinc finger motifs flanking the U2AF homology motif (UHM) domain. SRSF2 mutations exclusively occurred at P95 within an intervening sequence between the RNA recognition motif (RRM) and arginine/serine-rich (RS) domains (Fig. 2 and Supplementary Figs 8 and 9). Similarly, SF3B1 mutations predominantly involved K700 and, to a lesser extent, K666, H662 and E622, which are also conserved across species (Fig. 2 and Supplementary Fig. 10). The involvement of recurrent amino acid positions in these spliceosome genes strongly indicated a gain-of-function nature of these mutations, which has been a well-documented scenario in other oncogenic mutations[25]. On the other hand, the 23 mutations in *ZRSR2* (Xp22.1) were widely distributed along the entire coding region (Fig. 2). Among these, 14 mutations were nonsense or frameshift changes, or involved splicing donor/acceptor sites that caused either a premature truncation or a large structural change of the protein, leading to loss-of-function. Combined with their strong male preference for the mutation (14/14 cases), *ZRSR2* most likely acts as a tumour suppressor gene with an X-linked recessive mode of genetic action. The remaining nine *ZRSR2* mutations were missense changes and found in both males (six cases) and females (three cases), whose somatic origin was only confirmed in two cases. However, neither the dbSNP database (build131 and 132) nor the 1000 Genomes database (May 2011 snp calls) contained these missense nucleotides, suggesting that many, if not all, of these missense changes are likely to represent functional somatic changes, especially those found in males. Interrogation of these hot spots for mutations in *U2AF35* and *SRSF2* found no mutations among lymphoid neoplasms, including acute lymphoblastic leukaemia ($N = 24$) or non-Hodgkin's lymphoma ($N = 87$) (data not shown).

RNA splicing and spliceosome mutations

Because the splicing pathway mutations in myelodysplasia widely and specifically affect the major components of the splicing complexes E/A in a mutually exclusive manner, the common consequence of these mutations is logically the impaired recognition of 3′SSs that would lead to the production of aberrantly spliced mRNA species. To appreciate this and also to gain an insight into the biological/biochemical impact of these splicing mutations, we expressed the wild-type and the mutant (S34F) U2AF35 in HeLa cells using retrovirus-mediated gene transfer with enhanced green fluorescent protein (EGFP) marking (Fig. 4a and Supplementary Methods III) and examined their effects on gene expression in these cells using GeneChip Human genome U133 plus 2.0 arrays (Affymetrix), followed by gene set enrichment analysis (GSEA) (Supplementary Methods IV)[26]. Intriguingly, the GSEA disclosed a significant enrichment of the genes on the nonsense-mediated mRNA decay (NMD) pathway among the significantly upregulated genes in mutant *U2AF35*-transduced HeLa cells (Fig. 4b, Supplementary Fig. 11a and Supplementary Table 7), which was confirmed by quantitative polymerase chain reactions (qPCR) (Fig. 4c and Supplementary Methods 5V). A similar result was also observed for the gene expression profile of an MDS-derived cell line (TF-1) transduced with the S34F mutant (Supplementary Figs 11b, c). The NMD activation by the mutant U2AF35 was suppressed significantly by the co-overexpression of the wild-type protein (Supplementary Fig. 11d), indicating that the effect of the mutant protein was likely to be mediated by inhibition of the functions of the wild-type protein. Given that the NMD pathway, known as mRNA surveillance, provides a post-transcriptional mechanism for recognizing and eliminating abnormal transcripts that prematurely terminate translation[27], the result of the GSEA analyses indicated that the mutant U2AF35 induced abnormal RNA splicing in HeLa and TF-1 cells, leading to the generation of unspliced RNA species having a premature stop codon and induction of the NMD activity.

To confirm this, we next performed whole transcriptome analysis in these cells using the GeneChip Human exon 1.0 ST Array (Affymetrix), in which we differentially tracked the behaviour of two discrete sets of probes showing different level of evidence of being exons, that is, 'Core' (authentic exons) and 'non-Core' (more likely introns) sets (Supplementary Methods IV and Supplementary Fig. 12). As shown in Fig. 4d, the Core and non-Core set probes were differentially enriched among probes showing significant difference in expression between wild-type and mutant-transduced cells (false discovery rate (FDR) = 0.01). The Core set probes were significantly enriched in those probes significantly downregulated in mutant *U2AF35*-transduced cells compared with wild-type *U2AF35*-transduced cells, whereas the non-Core set probes were enriched in those probes significantly upregulated in mutant *U2AF35*-transduced cells (Fig. 4e). The significant differential enrichment was also demonstrated, even when all probe sets were included (Fig. 4f). Moreover, the significantly differentially expressed Core set probes tended to be up- and downregulated in wild-type and mutant *U2AF35*-transduced cells compared with mock-transduced cells, respectively, and vice versa for the differentially expressed non-Core set probes (Fig. 4e). Combined, these exon array results indicated that the wild-type U2AF35 correctly promoted authentic RNA splicing, whereas the mutant U2AF35 inhibited this processes, rendering non-Core and therefore, more likely intronic sequences to remain unspliced.

The abnormal splicing in mutant *U2AF35*-transduced cells was more directly demonstrated by sequencing mRNAs extracted from HeLa cells, in which expression of the wild-type and mutant (S34F) U2AF35 were induced by doxycycline. First, after adjusting by the total number of mapped reads, the wild-type *U2AF35*-transduced cells showed an increased read counts in the exon fraction, but reduced counts in other fractions, compared with mutant *U2AF35*-transduced cells (Fig. 4g). The reads from the mutant-transduced cells were mapped to broader genomic regions compared with those from the wild-type *U2AF35*-transduced cells, which were largely explained by non-exon reads (Fig. 4h). Finally, the number of those reads that encompassed the authentic exon/intron junctions was significantly increased in mutant *U2AF35*-transduced cells compared with wild-type *U2AF35*-transduced cells (Fig. 4i and Supplementary Methods VI). These results clearly demonstrated that failure of splicing ubiquitously occurred in mutant *U2AF35*-transduced cells. A typical example of abnormal splicing in mutant-transduced cells and the list of significantly unspliced exons are shown in Supplementary Fig. 13 and Supplementary Table 8, respectively.

Biological consequence of U2AF35 mutations

Finally, we examined the biological effects of compromised functions of the E/A splicing complexes. First, TF-1 and HeLa cells were transduced with lentivirus constructs expressing either the S34F U2AF35 mutant or wild-type U2AF35 under a tetracycline-inducible promoter (Fig. 5a and Supplementary Figs 14a and 15a), and cell proliferation was examined after the induction of their expression. Unexpectedly, after the induction of gene expression with doxycycline, the mutant *U2AF35*-transduced cells, but not the wild-type *U2AF35*-transduced cells, showed reduced cell proliferation (Fig. 5b and Supplementary Fig. 15b) with a marked increase in the G2/M fraction (G2/M arrest) together with enhanced apoptosis as

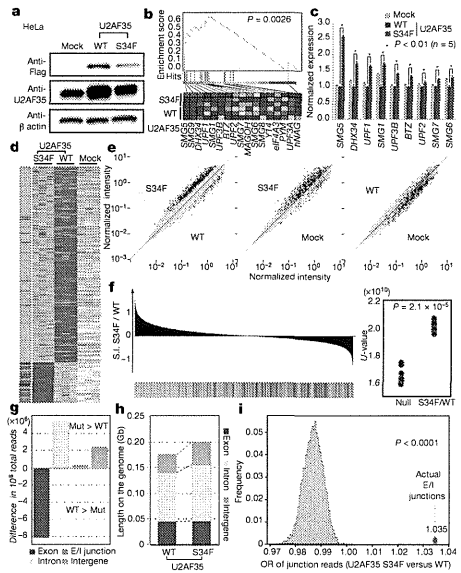

Figure 4 | Altered RNA splicing caused by a U2AF35 mutant. **a**, Western blot analyses showing expression of transduced wild-type or mutant (S34F) U2AF35 in HeLa cells used for the analyses of expression and exon microarrays. **b**, The GSEA demonstrating a significant enrichment of the set of 17 NMD pathway genes among significantly differentially expressed genes between wild-type and mutant *U2AF35*-transduced HeLa cells. The significance of the gene set was empirically determined by 1,000 gene-set permutations. **c**, The confirmation of the microarray analysis for the expression of nine genes that contributed to the core enrichment in the NMD gene set. Means ± s.e. are provided for the indicated NMD genes. *P* values were determined by the Mann–Whitney *U* test. **d**, Significantly upregulated and downregulated probe sets (FDR = 0.01) in mutant *U2AF35*-transduced cells compared with wild-type *U2AF35*-transduced cells in triplicate exon array experiments are shown in a heat map. The origin of each probe set is depicted in the left lane, where red and green bars indicate the Core and non-Core sets, respectively. **e**, Pair-wise scatter plots of the normalized intensities of entire probe sets (grey) across different experiments. The Core and non-Core set probes that were significantly differentially expressed between the wild-type and mutant *U2AF35*-transduced cells are plotted in red and green, respectively. **f**, Distribution of the Core (red) and non-Core (green) probe sets within the entire probe sets ordered by splicing index (S.I.; Supplementary Methods IV), calculated between wild-type and mutant *U2AF35*-transduced cells. In the right panel, the differential enrichment of both probe sets was confirmed by Mann–Whitney *U* test. **g**, Difference in read counts for the indicated fractions per 10^8 total reads in RNA sequencing between wild-type and mutant U2AF35-expressing HeLa cells analysis. Increased/decreased read counts in mutant U2AF35-expressing cells are plotted upward/downward, respectively. **h**, Comparison of the genome coverage by the indicated fractions in wild-type- and mutant-U2AF35-expressing cells. The genome coverage was calculated for each fraction within the 10^8 reads randomly selected from the total reads and averaged for ten independent selections. **i**, The odds ratio of the junction reads within the total mapped reads was calculated between the two experiments (red circle), which was evaluated against the 10,000 simulated values under the null hypothesis (histogram in blue).

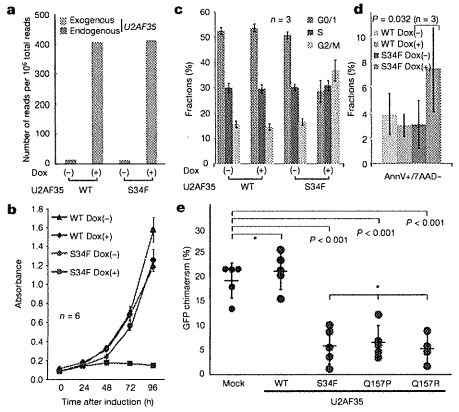

Figure 5 | Functional analysis of mutant U2AF35. a, Expression of endogenous and exogenous *U2AF35* transcripts in HeLa cells before and after induction determined by RNA sequencing. *U2AF35* transcripts were differentially enumerated for endogenous and exogenous species, which were discriminated by the Flag sequence. **b**, Cell proliferation assays of *U2AF35*-transduced HeLa cells, where cell numbers were measured using cell-counting apparatus and are plotted as mean absorbance ± s.d. **c**, The flow cytometry analysis of propidium iodide (PI)-stained HeLa cells transduced with the different U2AF35 constructs. Mean fractions ± s.d. in G0/G1, S and G2/M populations after the induction of U2AF35 expression are plotted. **d**, Fractions of the annexin V-positive (AnnV+) populations among the 7-amino-actinomycin D (7AAD)-negative population before and after the induction of U2AF35 expression are plotted as mean ± s.d. for indicated samples. The significance of difference was determined by paired *t*-test. **e**, Competitive reconstitution assays for CD34-negative KSL cells transduced with indicated U2AF35 mutants. Chimaerism in the peripheral blood 6 weeks after transplantation are plotted as mean %EGFP-positive Ly5.1 cells ± s.d., where outliers were excluded from the analysis. The significance of differences was evaluated by the Grubbs test with Bonferroni's correction for multiple testing. *not significant.

indicated by the increased sub-G1 fraction and annexin V-positive cells (Fig. 5c, d, Supplementary Fig. 14b and Supplementary Methods VI). To confirm the growth-suppressive effect of U2AF35 mutants *in vitro*, a highly purified haematopoietic stem cell population ($CD34^-$c-$Kit^+Scal^+Lin^-$, $CD34^-$KSL) prepared from C57BL/6 (B6)-Ly5.1 mouse bone marrow[28] was retrovirally transduced with either the mutant (S34F, Q157P and Q157R) or wild-type *U2AF35*, or the mock constructs, each harbouring the EGFP marker gene (Supplementary Fig. 16). The ability of these transduced cells to reconstitute the haematopoietic system was tested in a competitive reconstitution assay. The transduced cells were mixed with whole bone marrow cells from B6-Ly5.1/5.2 F1 mice, transplanted into lethally irradiated B6-Ly5.2 recipients, and peripheral blood chimaerism derived from EGFP-positive cells was assessed 6 weeks after transplantation by flow cytometry. We confirmed that each recipient mouse received comparable numbers of EGFP-positive cells among the different retrovirus groups by estimating the percentage of EGFP-positive cells and overall proliferation in transduced cells by *ex vivo* tracking. Also no significant difference was observed in their homing capacity to bone marrow as assessed by transwell migration assays (Supplementary Fig. 17). As shown in Fig. 5e, the wild-type *U2AF35*-transduced cells showed a slightly higher reconstitution capacity than the mock-transduced cells. On the other hand, the recipients of the cells transduced with the various *U2AF35* mutants showed significantly lower EGFP-positive cell chimaerism than those of either the mock- or the wild-type *U2AF35*-transduced cells, indicating a compromised reconstitution capacity of the haematopoietic stem/progenitor cells expressing the U2AF35 mutants. In summary, these mutants lead to loss-of-function of U2AF35 most probably by acting in a dominant-negative fashion to the wild-type protein.

Discussion

Our whole-exome sequencing study unexpectedly unmasked a complexity of novel pathway mutations found in approximately 45% to 85% of myelodysplasia patients depending on the disease subtypes, which affected multiple but distinctive components of the splicing machinery and, as such, demonstrated the unquestionable power of massively parallel sequencing technologies in cancer research.

The RNA splicing system comprises essential cellular machinery, through which eukaryotes can achieve successful transcription and guarantee the functional diversity of their protein species using alternative splicing in the face of a limited number of genes[29]. Accordingly, the meticulous regulation of this machinery should be indispensable for the maintenance of cellular homeostasis[30], deregulation of which causes severe developmental abnormalities[31,32]. The current discovery of frequent mutations of the splicing pathway in myelodysplasia, therefore, represents another remarkable example that illustrates how cancer develops by targeting critical cellular functions. It also provides an intriguing insight into the mechanism of 'cancer specific' alternative splicing, which have long been implicated in the development of cancer, including MDS and other haematopoietic neoplasms[33,34].

In myelodysplasia, the major targets of spliceosome mutations seemed to be largely confined to the components of the E/A splicing complex, among others to *SF3B1*, *SRSF2*, *U2AF35* and *ZRSR2*, and to a lesser extent, to *SF3A1*, *SF1*, *U2AF65* and *PRPF40B*. The broad coverage of the wide spectrum of spliceosome components in our exome sequencing was likely to preclude frequent involvement of other components on this pathway (Supplementary Fig. 18). The surprising frequency and specificity of these mutations in this complex, together with the mutually exclusive manner they occurred, unequivocally indicate that the compromised function of the E/A complex is a hallmark of this unique category of myeloid neoplasms, playing a central role in the pathogenesis of myelodysplasia. The close relationship between the mutation types and unique disease subtypes also support their pivotal roles in MDS.

Given the critical functions of the E/A splicing complex on the precise 3′SS recognition, the logical consequence of these relevant mutations would be the impaired splicing involving diverse RNA species. In fact, when expressed in HeLa cells, the mutant U2AF35 induced global abnormalities of RNA splicing, leading to increased production of transcripts having unspliced intronic sequences. On the other hand, the functional link between the abnormal splicing of RNA species and the phenotype of myelodysplasia is still unclear. Mutant U2AF35 seemed to suppress cell growth/proliferation and induce apoptosis rather than confer a growth advantage or promote clonal selection. *ZRSR2* knockdown in HeLa cells has been reported to also result in reduced viability, arguing for the common consequence of these pathway mutations[35]. These observations suggested that the oncogenic actions of these splicing pathway mutations are distinct from what is expected for classical oncogenes, such as mutated kinases and signal transducers, but could be more related to cell differentiation. Of note in this regard, the commonest clinical presentation of MDS is severe cytopenia in multiple cell lineages due to ineffective haematopoiesis with increased apoptosis rather than unlimited cell proliferation[1]. In this regard, lessons may be learned from the recent findings on the pathogenesis of the 5q− syndrome, where haploinsufficiency of *RPS14* leads to increased apoptosis of erythroid progenitors, but not myeloproliferation[36,37].

A lot of issues remain to be answered, however, to establish the functional link between these splicing pathway mutations and the pathogenesis of MDS, where the broad spectrum of RNA species affected by impaired splicing hampers identification of responsible gene targets. Moreover, the mutated components of the splicing machinery have distinct function of their own other than direct regulation of RNA splicing, involved in elongation and DNA stability, which may be important to determine specific disease phenotypes. Clearly, more studies are required to answer these questions through understanding of the molecular basis of their oncogenic actions.

METHODS SUMMARY

Whole-exome sequencing of paired tumour/normal DNA samples from the 29 patients was performed after informed consent was obtained. SNP array-based copy number analysis was performed as previously described[17,18]. Mutation analysis of the splicing pathway genes in a set of 582 myeloid neoplasms were performed by first screening mutations in PCR-amplified pooled targets from 12 individuals, followed by validation/identification of the candidate mutations within the corresponding 12 individuals by Sanger sequencing. Flag-tagged cDNAs of the wild-type and mutant *U2AF35* were generated by *in vitro* mutagenesis, constructed into a murine stem cell virus-based retroviral vector as well as a tetracycline-inducible lentivirus-based expression vector, and used for gene transfer to $CD34^-$KSL cells and cultured cell lines, with EGFP marking, respectively. Total RNA was extracted from wild-type or mutant *U2AF35*-transduced HeLa and TF-1 cells, and analysed on microarrays. RNA sequencing was performed according to the manufacturer's instructions (Illumina). Cell proliferation assays (MTT assays) on HeLa and TF-1 cells stably transduced with lentivirus U2AF35 constructs were performed in the presence or absence of doxycycline. For competitive reconstitution assays, $CD34^-$KSL cells collected from C57BL/6 (B6)-Ly5.1 mice were retrovirally transduced with various *U2AF35* constructs with EGFP marking, and transplanted with competitor cells (B6-Ly5.1/5.2 F1 mouse origin) into lethally irradiated B6-Ly5.2 mice 48 h after gene transduction. Frequency of EGFP-positive cells was assessed in peripheral blood by flow cytometry 6 weeks after the transplantation (Supplementary Methods VII). The primer sets used for validation of gene mutations and qPCR of NMD gene expression are listed in Supplementary Tables 9–11. A complete description of the materials and methods is provided in the Supplementary Information. This study was approved by the ethics boards of the University of Tokyo, Munich Leukaemia Laboratory, University Hospital Mannheim, University of Tsukuba, Tokyo Metropolitan Ohtsuka Hospital and Chang Gung Memorial Hospital. Animal experiments were performed with approval of the Animal Experiment Committee of the University of Tokyo.

Received 7 June; accepted 24 August 2011.
Published online 11 September 2011.

1. Corey, S. J. *et al.* Myelodysplastic syndromes: the complexity of stem-cell diseases. *Nature Rev. Cancer* **7,** 118–129 (2007).
2. Ma, X., Does, M., Raza, A. & Mayne, S. T. Myelodysplastic syndromes: incidence and survival in the United States. *Cancer* **109,** 1536–1542 (2007).
3. Bejar, R., Levine, R. & Ebert, B. L. Unraveling the molecular pathophysiology of myelodysplastic syndromes. *J. Clin. Oncol.* **29,** 504–515 (2011).
4. Sanada, M. *et al.* Gain-of-function of mutated *C-CBL* tumour suppressor in myeloid neoplasms. *Nature* **460,** 904–908 (2009).
5. Campbell, P. J. *et al.* Identification of somatically acquired rearrangements in cancer using genome-wide massively parallel paired-end sequencing. *Nature Genet.* **40,** 722–729 (2008).
6. Chapman, M. A. *et al.* Initial genome sequencing and analysis of multiple myeloma. *Nature* **471,** 467–472 (2011).
7. Lee, W. *et al.* The mutation spectrum revealed by paired genome sequences from a lung cancer patient. *Nature* **465,** 473–477 (2010).
8. Ley, T. J. *et al.* DNA sequencing of a cytogenetically normal acute myeloid leukaemia genome. *Nature* **456,** 66–72 (2008).
9. Metzker, M. L. Sequencing technologies — the next generation. *Nature Rev. Genet.* **11,** 31–46 (2010).
10. Shendure, J. & Ji, H. Next-generation DNA sequencing. *Nature Biotechnol.* **26,** 1135–1145 (2008).
11. Shah, S. P. *et al.* Mutational evolution in a lobular breast tumour profiled at single nucleotide resolution. *Nature* **461,** 809–813 (2009).
12. Varela, I. *et al.* Exome sequencing identifies frequent mutation of the SWI/SNF complex gene *PBRM1* in renal carcinoma. *Nature* **469,** 539–542 (2011).
13. Ley, T. J. *et al. DNMT3A* mutations in acute myeloid leukemia. *N. Engl. J. Med.* **363,** 2424–2433 (2010).
14. Mardis, E. R. *et al.* Recurring mutations found by sequencing an acute myeloid leukemia genome. *N. Engl. J. Med.* **361,** 1058–1066 (2009).
15. Yan, X. J. *et al.* Exome sequencing identifies somatic mutations of DNA methyltransferase gene *DNMT3A* in acute monocytic leukemia. *Nature Genet.* **43,** 309–315 (2011).
16. Puente, X. S. *et al.* Whole-genome sequencing identifies recurrent mutations in chronic lymphocytic leukaemia. *Nature* **475,** 101–105 (2011).
17. Nannya, Y. *et al.* A robust algorithm for copy number detection using high-density oligonucleotide single nucleotide polymorphism genotyping arrays. *Cancer Res.* **65,** 6071–6079 (2005).
18. Yamamoto, G. *et al.* Highly sensitive method for genomewide detection of allelic composition in nonpaired, primary tumor specimens by use of Affymetrix single-nucleotide-polymorphism genotyping microarrays. *Am. J. Hum. Genet.* **81,** 114–126 (2007).
19. Wahl, M. C., Will, C. L. & Luhrmann, R. The spliceosome: design principles of a dynamic RNP machine. *Cell* **136,** 701–718 (2009).
20. Tronchère, H., Wang, J. & Fu, X. D. A protein related to splicing factor $U2AF^{35}$ that interacts with $U2AF^{65}$ and SR proteins in splicing of pre-mRNA. *Nature* **388,** 397–400 (1997).
21. Bevilacqua, L. *et al.* A population-specific *HTR2B* stop codon predisposes to severe impulsivity. *Nature* **468,** 1061–1066 (2010).
22. Calvo, S. E. *et al.* High-throughput, pooled sequencing identifies mutations in *NUBPL* and *FOXRED1* in human complex I deficiency. *Nature Genet.* **42,** 851–858 (2010).
23. Haase, D. *et al.* New insights into the prognostic impact of the karyotype in MDS and correlation with subtypes: evidence from a core dataset of 2124 patients. *Blood* **110,** 4385–4395 (2007).
24. Xiao, R. *et al.* Splicing regulator SC35 is essential for genomic stability and cell proliferation during mammalian organogenesis. *Mol. Cell. Biol.* **27,** 5393–5402 (2007).
25. Morin, R. D. *et al.* Somatic mutations altering EZH2 (Tyr641) in follicular and diffuse large B-cell lymphomas of germinal-center origin. *Nature Genet.* **42,** 181–185 (2010).
26. Subramanian, A. *et al.* Gene set enrichment analysis: a knowledge-based approach for interpreting genome-wide expression profiles. *Proc. Natl Acad. Sci. USA* **102,** 15545–15550 (2005).
27. Maquat, L. E. Nonsense-mediated mRNA decay: splicing, translation and mRNP dynamics. *Nature Rev. Mol. Cell Biol.* **5,** 89–99 (2004).
28. Ema, H. *et al.* Adult mouse hematopoietic stem cells: purification and single-cell assays. *Nature Protocols* **1,** 2979–2987 (2007).
29. Chen, M. & Manley, J. L. Mechanisms of alternative splicing regulation: insights from molecular and genomics approaches. *Nature Rev. Mol. Cell Biol.* **10,** 741–754 (2009).
30. Ni, J. Z. *et al.* Ultraconserved elements are associated with homeostatic control of splicing regulators by alternative splicing and nonsense-mediated decay. *Genes Dev.* **21,** 708–718 (2007).
31. He, H. *et al.* Mutations in U4atac snRNA, a component of the minor spliceosome, in the developmental disorder MOPD I. *Science* **332,** 238–240 (2011).
32. Edery, P. *et al.* Association of TALS developmental disorder with defect in minor splicing component *U4atac* snRNA. *Science* **332,** 240–243 (2011).
33. David, C. J. & Manley, J. L. Alternative pre-mRNA splicing regulation in cancer: pathways and programs unhinged. *Genes Dev.* **24,** 2343–2364 (2010).
34. Pajares, M. J. *et al.* Alternative splicing: an emerging topic in molecular and clinical oncology. *Lancet Oncol.* **8,** 349–357 (2007).
35. Shen, H., Zheng, X., Luecke, S. & Green, M. R. The U2AF35-related protein Urp contacts the 3′ splice site to promote U12-type intron splicing and the second step of U2-type intron splicing. *Genes Dev.* **24,** 2389–2394 (2010).
36. Barlow, J. L. *et al.* A p53-dependent mechanism underlies macrocytic anemia in a mouse model of human 5q− syndrome. *Nature Med.* **16,** 59–66 (2010).
37. Ebert, B. L. *et al.* Identification of *RPS14* as a $5q^-$ syndrome gene by RNA interference screen. *Nature* **451,** 335–339 (2008).

Supplementary Information is linked to the online version of the paper at www.nature.com/nature.

Acknowledgements This work was supported by Grant-in-Aids from the Ministry of Health, Labor and Welfare of Japan and from the Ministry of Education, Culture, Sports, Science and Technology, and also by the Japan Society for the Promotion of Science (JSPS) through the 'Funding Program for World-Leading Innovative R&D on Science and Technology (FIRST Program)', initiated by the Council for Science and Technology Policy (CSTP). pGCDNsamIRESEGFP vector was a gift from M. Onodera. We thank Y. Mori, O. Hagiwara, M. Nakamura and N. Mizota for their technical assistance. We are also grateful to K. Ikeuchi and M. Ueda for their continuous encouragement throughout the study.

Author Contributions Y.Sh., Y.Sa., A.S.-O., Y.N., M.N., G.C., R.K. and S.Miyano were committed to bioinformatics analyses of resequencing data. M.Sa., A.S.-O. and Y.Sa. performed microarray experiments and their analyses. R.Y., T.Y., M.O., M.Sa., A.K., M.Sh. and H.N. were involved in the functional analyses of U2AF35 mutants. N.O., M.S.-Y., K.I., H.M., W.-K.H., F.N., D.N., T.H., C.H., S.Miyawaki, S.C., H.P.K. and L.-Y.S. collected specimens and were also involved in planning the project. K.Y., Y.N., Y.Su., A.S.-O. and S.S. processed and analysed genetic materials, library preparation and sequencing. K.Y., M.Sa., Y.Sh., A.S.-O., Y. Sa. and S.O. generated figures and tables. S.O. led the entire project and wrote the manuscript. All authors participated in the discussion and interpretation of the data and the results.

Author Information Sequence data have been deposited in the DDBJ repository under accession number DRA000433. Microarray data have been deposited in the GEO database under accession numbers GSE31174 (for SNP arrays), GSE31171 (for exon arrays) and GSE31172 (for expression arrays). Reprints and permissions information is available at www.nature.com/reprints. The authors declare no competing financial interests. Readers are welcome to comment on the online version of this article at www.nature.com/nature. Correspondence and requests for materials should be addressed to S.O. (sogawa-tky@umin.ac.jp).

Brief report

Heterozygous *ITGA2B* R995W mutation inducing constitutive activation of the αIIbβ3 receptor affects proplatelet formation and causes congenital macrothrombocytopenia

Shinji Kunishima,[1] Hirokazu Kashiwagi,[2] Makoto Otsu,[3] Naoya Takayama,[3] Koji Eto,[3] Masafumi Onodera,[4] Yuji Miyajima,[5] Yasushi Takamatsu,[6] Junji Suzumiya,[7] Kousaku Matsubara,[8] Yoshiaki Tomiyama,[2,9] and Hidehiko Saito[10]

[1]Department of Advanced Diagnosis, Clinical Research Center, National Hospital Organization Nagoya Medical Center, Nagoya, Japan; [2]Department of Hematology and Oncology, Graduate School of Medicine, Osaka University, Osaka, Japan; [3]Division of Stem Cell Therapy, Center for Stem Cell and Regenerative Medicine, Institute of Medical Science, University of Tokyo, Tokyo, Japan; [4]Department of Genetics, National Research Institute for Child Health and Development, Tokyo, Japan; [5]Department of Pediatrics, Anjo Kosei Hospital, Anjo, Japan; [6]Department of Medical Oncology, Hematology and Infectious Disease, Fukuoka University, Fukuoka, Japan; [7]Shimane University Hospital Cancer Center, Shimane, Japan; [8]Department of Pediatrics, Nishi-Kobe Medical Center, Kobe, Japan; [9]Department of Blood Transfusion, Osaka University Hospital, Osaka, Japan; and [10]Nagoya Central Hospital, Nagoya, Japan

Congenital macrothrombocytopenia is a genetically heterogeneous group of rare disorders. αIIbβ3 has not been implicated in these conditions. We identified a novel, conserved heterozygous *ITGA2B* R995W mutation in 4 unrelated families. The surface expression of platelet αIIbβ3 was decreased to 50% to 70% of control. There was spontaneous PAC-1 and fibrinogen binding to resting platelets without CD62p expression. The activation state of αIIbβ3 in 293T cells was higher for αIIb-W995 than for β3-H723 but was weaker than for β3-N562. FAK was spontaneously phosphorylated in αIIb-W995/β3-transfected 293T cells. These results indicate that αIIb-W995/β3 has a constitutive, activated conformation but does not induce platelet activation. αIIb-W995/β3-transfected CHO cells developed membrane ruffling and abnormal cytoplasmic protrusions. The increased size and decreased number of proplatelet tips in αIIb-W995/β3-transduced mouse fetal liver-derived megakaryocytes indicate defective proplatelet formation. We propose that activating mutations in *ITGA2B* and *ITGB3* represent the etiology of a subset of congenital macrothrombocytopenias. (*Blood*. 2011;117(20):5479-5484)

Introduction

Congenital macrothrombocytopenia is a genetically heterogeneous group of rare disorders.[1-4] The most frequent forms include *MYH9* disorders and Bernard-Soulier syndrome. In approximately half of cases of congenital macrothrombocytopenia, the pathogenesis remains unknown; thus, a definite diagnosis is unavailable. Glanzmann thrombasthenia is the most common congenital platelet disorder caused by qualitative or quantitative abnormality of the integrin αIIbβ3, in which the platelet counts and morphology are normal.[5] However, *ITGA2B* R995Q mutation has been reported in a patient with Glanzmann thrombasthenia-like phenotype and macrothrombocytopenia.[6,7] Recently, heterozygous *ITGB3* mutations were found in patients with congenital macrothrombocytopenia.[8-10] We report here a novel, conserved heterozygous *ITGA2B* R995W mutation in 4 unrelated families.

Methods

Patients

Twenty-seven patients with congenital macrothrombocytopenia, in whom *MYH9* disorders, heterozygous and homozygous Bernard-Soulier syndrome, type 2B von Willebrand disease, and *TUBB1* mutations were excluded, underwent mutational analysis of *ITGA2B* and *ITGB3*. Fifty-five consecutive patients were prospectively analyzed for the surface expression of platelet αIIbβ3. Written informed consent was obtained from all patients or their parents in accordance with the Declaration of Helsinki. Institutional review boards of Nagoya Medical Center and each of the participating institutions/hospitals approved this study.

Genetic analysis

The entire coding sequence of exons and exon-intron boundaries of *ITGA2B* (supplemental Table 1, available on the *Blood* Web site; see the Supplemental Materials link at the top of the online article) and *ITGB3* was amplified by polymerase chain reaction and sequenced. The disease-associated *ITGA2B* haplotype was determined by cloning and sequencing the polymerase chain reaction products.

Platelet glycoprotein analysis

Flow cytometry and immunoblotting were performed as described previously.[11,12] The activation state of αIIbβ3 was evaluated by the binding of the ligand-mimetic antibody PAC-1 (BD Biosciences) and FITC-labeled fibrinogen.[13]

Cloning, mutagenesis, and retroviral transduction

ITGA2B and *ITGB3* sequences were amplified from the patient's platelet cDNA and cloned into pcDNA3.1 (Invitrogen). T562N[13] and D723H[8] were introduced into *ITGB3* cDNA using site-directed mutagenesis. *ITGA2B* and *ITGB3* expression plasmids were cotransfected into 293T and CHO cells.

Submitted December 7, 2010; accepted March 18, 2011. Prepublished online as *Blood* First Edition paper, March 31, 2011; DOI 10.1182/blood-2010-12-323691.

The online version of this article contains a data supplement.

The publication costs of this article were defrayed in part by page charge payment. Therefore, and solely to indicate this fact, this article is hereby marked "advertisement" in accordance with 18 USC section 1734.

From bloodjournal.hematologylibrary.org at Nagoya Medical Center on May 19, 2011. For personal use only.

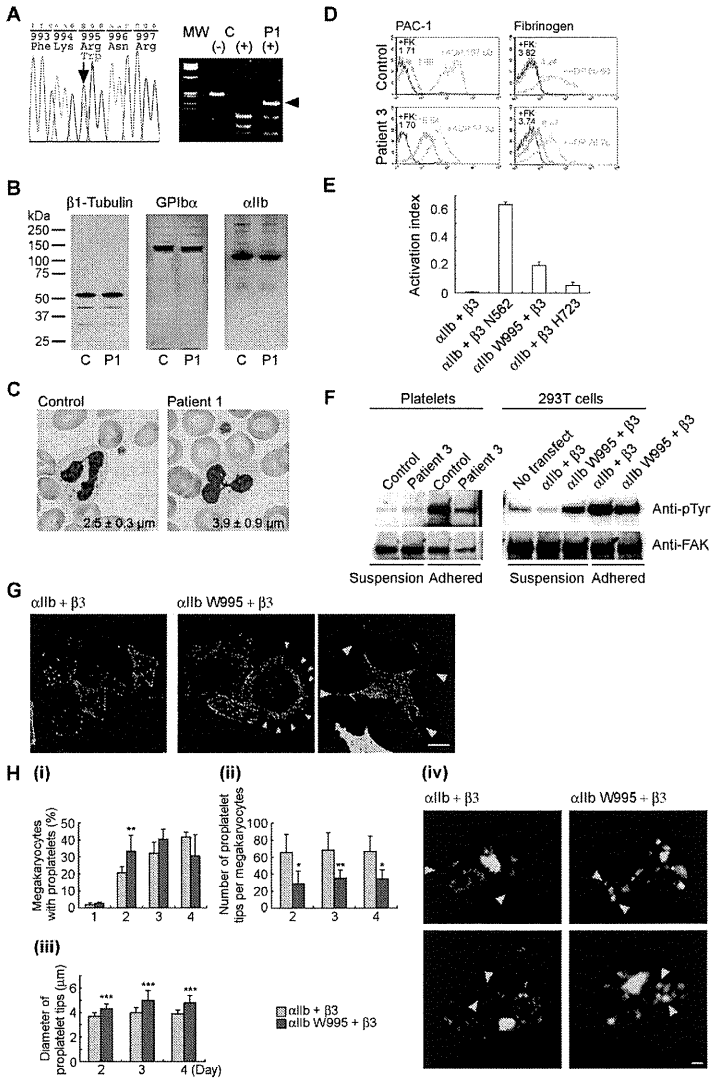

Figure 1. Platelet morphology and biochemical, genetic, and functional analyses of *ITGA2B* R995W mutation. (A; left) DNA sequence analysis of *ITGA2B*. The entire coding regions of the patients' *ITGA2B* were amplified from genomic DNA by the polymerase chain reaction, and amplified DNA fragments were subjected to direct cycle sequence analysis. A C to T transition at nucleotide 3077, changing Arg995 to Trp (R995W), was detected. Nucleotide numbering for *ITGA2B* cDNA is according to Poncz et al.[18] The arrow shows the position of the substitution. (Right) Allele-specific restriction analysis. DNA fragments amplified using primers 2Bg305/303 (supplemental Table 1) were digested with BspACI (SibEnzyme), electrophoresed on 2% agarose gels, and stained with ethidium bromide. The 3077C > T substitution abolishes a recognition site for BspACI, generating a new 231-bp band (arrowhead). The mutation was not found in 108 healthy controls or in the SNP database (www.ncbi.nlm.nih.gov/SNP). MW indicates HaeIII digest of ΦX 174 DNA; C, control; and P1, patient 1. (B) Immunoblot analysis of platelets. Triton X-100-soluble platelet lysates were separated by sodium dodecyl sulfate-polyacrylamide gel electrophoresis on 4% to 12% gradient acrylamide slab gels (Invitrogen) and electroblotted onto polyvinylidine difluoride membranes. The blots were incubated with anti-β1 tubulin antibody NB2301,[19] anti-GPIbα antibody PL524 (Takara), and anti-αIIb antibody SZ22 (Beckman-Coulter) and reacted with horseradish peroxidase-conjugated secondary antibody. The bound antibodies were visualized using an enhanced chemiluminescent substrate. C indicates control; and P1, patient 1.

Transfected cells were subjected to flow cytometry, FAK phosphorylation, and spreading assay.[13,14]

ITGA2B and *ITGB3* cDNAs were inserted upstream of internal ribosome entry site (IRES)-enhanced green fluorescent protein (EGFP) and IRES-Kusabira-Orange in the retroviral vector pGCDNsamIRES/EGFP and pGCDNsamIRES/huKO, respectively.[15,16] Each plasmid was transfected into 293gp packaging cells with a vesicular stomatitis virus G expression plasmid. Supernatants were used for the transduction of 293gpg producer cells harboring a tetracycline-inducible vesicular stomatitis virus G expression cassette,[17] and virus-bearing supernatant was harvested under tetracycline-deficient conditions.

Mouse fetal liver cells were harvested from embryonic day 13.5 embryos and cultured in Dulbecco modified Eagle medium supplemented with 10% fetal calf serum and 50 ng/mL human thrombopoietin. The next day, cells were infected with retroviruses expressing *ITGA2B* and *ITGB3* on recombinant human fibronectin fragment CH-296 (RetroNectin, Takara)-coated plates. After transduction, proplatelet formation was monitored for the next 4 days on EGFP and Kusabira-Orange double-positive megakaryocytes in suspension by inverted fluorescence microscopy. The Experimental Animal Committee of Nagoya Medical Center approved the animal studies.

Results and discussion

We searched for *ITGA2B* and *ITGB3* mutations in 27 patients with macrothrombocytopenia and identified a novel, conserved heterozygous *ITGA2B* R995W mutation in one patient (patient 1; Figure 1A). The decreased surface expression of platelet αIIbβ3 prompted us to prospectively screen its expression by flow cytometry. We detected decreased αIIbβ3 expression level (50%-70% of control) in 3 of 55 consecutive patients with macrothrombocytopenia of unknown etiology (patients 2-4 in Table 1). Immunoblotting showed a normal electrophoretic mobility of αIIb, but the total expression level relative to β1-tubulin was decreased to 0.7 (Figure 1B; Table 1). Sequence analysis identified the same heterozygous *ITGA2B* R995W mutation. In total, we identified 11 patients in 4 unrelated Japanese families. In each family, the disease-associated *ITGA2B* haplotype was unique, indicating independent occurrence (supplemental Table 2). Patients had larger platelets, approximately 30% increase of control, and moderate thrombocytopenia (Figure 1C; Table 1). These results indicate that macrothrombocytopenia shows a dominant inheritance.

Bleeding tendency was absent or mild (eg, patient 1 had undergone total colectomy without platelet transfusion). Platelet aggregation induced by adenosine diphosphate and collagen was reduced, although the bleeding time was within the normal limit (Table 1). Platelet spreading on immobilized fibrinogen was partially impaired: the number of fully spread platelets was decreased (supplemental Figure 1). These findings indicate that patients are asymptomatic or exhibit a marginal bleeding tendency and that the clinical and laboratory phenotype is distinct from Glanzmann thrombasthenia.

There was spontaneous PAC-1 binding to resting patients' platelets as well as to αIIb-W995/β3-transfected 293T cells. Although fibrinogen did not bind to platelets in whole blood, increased fibrinogen binding to the washed platelets was observed (Figure 1D; supplemental Figure 2). The activation state, quantified as an activation index in 293T cells, was higher for αIIb-W995 than for β3-H723 but was weaker than that for a strong activating mutant, β3-N562[13](Figure 1E). CD62p expression was absent on the resting platelets (supplemental Figure 2). Spontaneously phosphorylated FAK, a downstream effector of integrin signaling, was not evident in resting platelets in suspension, probably because of low expression level of abnormal αIIbβ3 receptor. However, FAK phosphorylation occurred in αIIb-W995/β3-transfected 293T cells in suspension, indicating constitutively activated αIIbβ3 (Figure 1F). These results indicate that R995W mutation changes αIIbβ3 to a constitutively, albeit partially, activated conformation, but does not induce platelet activation.

αIIb-R995 forms a salt bridge with β3-D723 in the membrane-proximal region and maintains the inactive conformation of the αIIbβ3.[20,21] Disruption of the interaction because of partially activated αIIb/β3-H723 or αIIb/β3-A723 mutants but not fully activated mutants, such as αIIb/β3-N562, was reported to cause microtubule-dependent abnormal proplatelet-like cytoplasmic extensions in megakaryocytes and CHO cells.[8,22] We found that

Figure 1. (continued) (C) Platelet morphology. Peripheral blood smears were stained with May-Grünwald-Giemsa for a normal control and patient 1 (original magnification, × 1000). The patient showed giant platelets with morphologically normal leukocytes. The number in each panel shows the mean platelet size (n = 200). Images were obtained using a BX50 microscope with a 100×/1.35 numeric aperture oil objective (Olympus). Images of the slides were acquired using a DP70 digital camera and DP manager software Version 1.2.1.107 (Olympus). (D) Activation state of platelet αIIbβ3. Washed platelets from patient 3 were resuspended in Tyrode buffer (137mM NaCl, 2.7mM KCl, 1.0mM $MgCl_2$, 3.3mM NaH_2PO_4, 3.8mM N-2-hydroxyethylpiperazine-N'-2-ethanesulfonic acid, 0.1% glucose, 0.1% bovine serum albumin, pH 7.4) and incubated with fluorescein isothiocyanate-conjugated PAC-1 or 125 μg/mL fluorescein isothiocyanate-labeled fibrinogen in the presence or absence of 10μM FK633 (αIIbβ3-specific peptidomimetic antagonist: black lines) or 10μM adenosine diphosphate (blue lines), and analyzed by flow cytometry. Numbers indicate the mean fluorescence intensity. Results are representative of 2 independent experiments. (E) Quantitation of the αIIbβ3 activation state. The activation state of αIIbβ3 was quantified as an activation index on transiently transfected 293T cells. The activation index was higher for αIIb-W995 than for β3-H723 but was weaker than for an activating mutant β3-N562. Activation index = (a − b)/(c − b), in which a is the mean fluorescence intensity of PAC-1 binding with buffer, b is the mean fluorescence intensity in the presence of FK633, and c is the mean fluorescence intensity in the presence of PT25–2 (anti-αIIbβ3 antibody, which induces the active conformation of αIIbβ3). Data are mean plus or minus SE (n = 3). (F) FAK phosphorylation. Washed platelets from patient 3 (left) or transiently transfected 293T cells (right) were incubated in suspension or seeded onto 100-μg/mL fibrinogen-coated plastic dishes for 1 hour. Cells were washed with phosphate-buffered saline and lysed with 1% Triton X-100 and 1mM sodium vanadate. FAK was immunoprecipitated from the lysates with anti-FAK antibody FAK(C903; Santa Cruz Biotechnology) and protein G-Sepharose, and phosphotyrosine was detected with the antiphosphotyrosine antibody 4G10 (Millipore). Note that 300-μg and 150-μg lysates from suspension and adhered platelets, respectively, and 200-μg lysates from suspension and adhered transfected 293T cells were used for immunoprecipitation analysis. To monitor the loading of gel lanes, the membrane was stripped and reprobed with the anti-FAK antibody FAK(A17; Santa Cruz Biotechnology). Results are representative of 2 and 3 independent experiments for platelets and transfected cells, respectively. (G) Abnormal cytoplasmic protrusions in αIIb-W995/β3-transfected CHO cells. Stably transfected CHO cells were seeded onto 100 μg/mL fibrinogen-coated glass coverslips and incubated for 2 hours at 37°C. Cells were fixed with 3.7% formaldehyde and permeabilized with 0.2% Triton X-100. Coverslips were then stained with anti-CD41a antibody HIP8 (BD Biosciences) followed by Alexa-488-labeled goat antimouse IgG (Invitrogen) and tetramethylrhodamine isothiocyanate-phalloidin (Sigma-Aldrich). Images were obtained using a confocal microscope with a Plan-Apochromat 63×/1.4 oil DIC objective lens LSM5Pascal (Carl Zeiss). Arrowheads indicate membrane ruffling (middle panel) and abnormal cytoplasmic protrusions with the bulbous tips (right panel) in αIIb-W995/β3-transfected CHO cells. Representative images from 3 independent experiments are shown. (H) Abnormal proplatelet formation in αIIb-W995/β3-transfected megakaryocytes. Mouse fetal liver-derived megakaryocytes infected with EGFP-αIIb and Kusabira-Orange-β3 retrovirus were examined in suspension cultures under an IX71 fluorescence microscope with an LCPlanFl 40×/0.60 objective lens (Olympus). (i) The percentage of megakaryocytes extending proplatelets was evaluated manually under a fluorescence microscope 1 to 4 days after infection. For each specimen, at least 100 megakaryocytes were evaluated. The number of proplatelet tips per megakaryocyte (ii) and the size of the proplatelet tips (iii) were measured on acquired images by the ImageScope software Version 10.2.2 (Aperio Technologies). At least 10 megakaryocytes were analyzed for each sample. An unpaired, 2-tailed *t* test was used to analyze data. A value of *P* less than .05 was considered statistically significant. Data are mean plus or minus SD. *$P < .05$. **$P < .01$. ***$P < .0001$. (iv) Representative megakaryocytes from 3 independent experiments are shown. Note that the number of proplatelet tips/bulbous structures (arrowheads) is decreased and the size of the tips increased in αIIb-W995/β3-transfected megakaryocytes than in wild-type αIIb/β3-transfected megakaryocytes. Scale bar represents 10 μm.

Table 1. Platelet characteristics of patients with the *ITGA2B* R995W mutation

Patient	Sex	Age, y	*ITGA2B* mutation	Platelet count, × 10⁴/L	Platelet size, μm†	Surface expression relative to control platelets, %‡					αIIb/β1 tubulin ratio to control§§	Duke bleeding time, minutes‖	Platelet aggregation¶			Bleeding tendency	Initial diagnosis
						αIIb	β3	αIIbβ3	GPIbα	GPIX			ADP, %	Collagen (2.0 μg/mL), %	Ristocetin (1.3 mg/mL), %		
Family 1																	
Patient 1	Male	55	R995W	65	3.9 ± 0.9	53.8	67.0	—	143.1	143.8	0.82	4.5	11 (3μM)	28	77	–	Unknown thrombocytopenia
Family 2																	
Father	Male	46	R995W	79	3.3 ± 0.9	51.3	51.4	56.5	106.7	109.8	—	—	—	—	—	–	—
Patient 2	Male	4	R995W	82	3.6 ± 1.0	54.0	58.6	61.8	138.3	134.7	0.75	5	—	—	—	Epistaxis	Congenital thrombocytopenia
Sister	Female	9	R995W	85	3.4 ± 1.0	55.6	60.6	68.4	120.0	133.1	0.71	3.5	—	—	—	–	—
Family 3																	
Mother	Female	56	R995W	80	2.8 ± 0.8	58.4	63.4	65.8	116.5	—	0.73	—				–	—
Patient 3	Female	27	R995W	74	3.5 ± 1.0	64.4	69.7	63.8	124.8	—	—	—	43 (10μM)	44	72	–	cITP
Sister	Female	24	R995W	100	3.6 ± 1.0	59.3	70.2	70.8	110.9	—	0.63	—	—	—	—	–	—
Family 4																	
Maternal grandfather	Male	58	R995W	66	3.4 ± 0.9	—	—	—	—	—	0.63	—	20 (3μM)	9	—	Hemorrhage in exodontia	—
Mother	Female	30	R995W	66	2.8 ± 0.8	56.3	62.5	57.5	127.2	112.1	0.63	2.5	—	—		Purpura, hemorrhage in exodontia	cITP
Patient 4	Female	4M	R995W	82	3.2 ± 1.0	63.3	62.9	62.3	147.7	140.5	0.63	—	23 (3μM)	11	—	–	NAITP
Brother	Male	5	R995W	122	3.1 ± 0.8	—	—	—	—	—	—	—	—	—	—	–	—
Mean ± SD				81.9 ± 16.8#	3.3 ± 0.3#	57.4 ± 4.4***	62.9 ± 5.8**	63.3 ± 5.0**	126.1 ± 14.3**	129.0 ± 14.5**	0.7 ± 0.07#						

— indicates not applicable; ADP, adenosine diphosphate; cITP, chronic immune thrombocytopenia; and NAITP, neonatal alloimmune thrombocytopenic purpura.

*Controls, 273.5 ± 60.4 (× 10^4/L) (n = 1014).

†Determined by microscopic observation of 200 platelets on a stained peripheral blood smear. Controls, 2.5 ± 0.3 μm (n = 31).

‡Platelets were reacted with fluorescein isothiocyanate-labeled monoclonal antibodies against αIIb (5B12; Dako Denmark), β3 (SZ21), αIIbβ3 (P2), GPIbα (SZ2; Beckman-Coulter), or GPIX (ALMA16. BD Biosciences) and analyzed in an Epics XL flow cytometer (Beckman-Coulter). Values are expressed as percentage of mean fluorescence intensities of control platelets.

§Platelet αIIbβ1-tubulin ratio was determined by densitometric analysis of immunoblots using ImageQuant software Version 5.0 (Molecular Dynamics).

‖Normal range, 2 to 5 minutes.

¶Platelet aggregation was performed in platelet-rich plasma. Results are given as percentage maximum aggregation.

#$P < .001$, **$P < .0001$ vs controls (2-tailed *t* test).

αIIb-W995/β3-transfected CHO cells exhibited membrane ruffling and abnormal cytoplasmic protrusions with the bulbous tips on fibrinogen-coated surfaces (Figure 1G), indicating that the salt bridge-disrupting mutations exert the same influence on the integrin activation and cytoskeletal events. Abnormal clustering of αIIbβ3, which was reported in *ITGB3* L718P mutation,[10] was not observed in these cells or in platelets spread on immobilized fibrinogen (supplemental Figure 1). It is worth noting that macrothrombocytopenia-associated *ITGB3* mutations in the ectodomain and the cytoplasmic membrane-proximal region have different properties in terms of outside-in signaling and bleeding tendency.[9,10]

Finally, to determine the functional consequences of R995W mutation on platelet production, we coexpressed αIIb and β3 in mouse fetal liver cells by retroviral transfer and differentiated them into megakaryocytes (Figure 1H). There was an early increase and decrease in the percentage of proplatelet formation-positive megakaryocytes in αIIb-W995/β3-transfected megakaryocytes. The number of proplatelet tips was decreased, and the size of the tips increased. These results are consistent with thrombocytopenia and the increased platelet size in patients, indicating that the stimulation of mutant αIIbβ3 leads to abnormal proplatelet formation. However, not all *ITGA2B*- and *ITGB3*-activating mutations are associated with macrothrombocytopenia. Patients with homozygous *ITGB3* C549R or C560R mutation inducing constitutively active αIIbβ3 have a normal platelet count and size,[23,24] suggesting different molecular mechanisms for the induction of abnormal proplatelet formation.

αIIbβ3 has not been implicated in an abnormal platelet count or morphology.[5] Our data support and extend the recent reports that heterozygous, activating mutations in *ITGA2B* and *ITGB3*, in the juxtamembrane region, cause macrothrombocytopenia.[6-10] We thus propose that such mutations represent the etiology of a subset of congenital macrothrombocytopenias. It is also probable that homozygosity causes Glanzmann thrombasthenia, as demonstrated in the original report of macrothrombocytopenia-associated *ITGA2B* R995Q mutation.[6,7] The creation of a knock-in mouse model and/or use of an in vivo megakaryocyte infusion model[25] should clarify the mechanism underlying the production and processing of giant platelets.

Acknowledgments

The authors thank Dr R. C. Mulligan (Children's Hospital Boston, Harvard Medical School, Boston, MA) for 293gp and 293gpg cells, Dr M. Handa (Department of Transfusion Medicine & Cell Therapy, Keio University School of Medicine, Tokyo, Japan) for PT25-2 antibodies, Dr A. Saito (Department of Clinical Research Promotion, Clinical Research Center, National Hospital Organization Nagoya Medical Center) for statistical analysis, and Yoshimi Ito-Yamamura for her skillful technical assistance.

This work was supported by the Japan Society for the Promotion of Science (Grant-in-Aid for Scientific Research), the Ministry of Health, Labor and Welfare, Academic Frontier Project in Japan, Mitsubishi Pharma Research Foundation, the 24th General Assembly of the Japanese Association of Medical Sciences Promotion Fund, the Mother and Child Health Foundation, and the National Hospital Organization Research Fund.

Authorship

Contribution: S.K. designed and performed research, analyzed data, and wrote the paper; H.K. and Y. Tomiyama performed platelet experiments and interpreted the results; M. Onodera constructed retrovirus vectors; M. Otsu, N.T., K.E., and M. Onodera designed the retroviral transfection experiments; Y.M., Y. Takamatsu, J.S., and K.M. contributed patient samples; and H.S. supervised the research.

Conflict-of-interest disclosure: The authors declare no competing financial interests.

Correspondence: Shinji Kunishima, Department of Advanced Diagnosis, Clinical Research Center, National Hospital Organization Nagoya Medical Center, 4-1-1 Sannomaru, Naka-ku, Nagoya 4600001, Japan; e-mail: kunishis@nnh.hosp.go.jp.

References

1. Balduini CL, Cattaneo M, Fabris F, et al. Inherited thrombocytopenias: a proposed diagnostic algorithm from the Italian Gruppo di Studio delle Piastrine. *Haematologica.* 2003;88(5): 582-592.
2. Balduini CL, Savoia A. Inherited thrombocytopenias: molecular mechanisms. *Semin Thromb Hemost.* 2004;30(5):513-523.
3. Kunishima S, Saito H. Congenital macrothrombocytopenias. *Blood Rev.* 2006;20(2):111-121.
4. Nurden P, Nurden AT. Congenital disorders associated with platelet dysfunctions. *Thromb Haemost.* 2008;99(2):253-263.
5. Nurden AT. Glanzmann thrombasthenia. *Orphanet J Rare Dis.* 2006;1:10.
6. Hardisty R, Pidard D, Cox A, et al. A defect of platelet aggregation associated with an abnormal distribution of glycoprotein IIb-IIIa complexes within the platelet: the cause of a lifelong bleeding disorder. *Blood.* 1992;80(3): 696-708.
7. Peyruchaud O, Nurden AT, Milet S, et al. R to Q amino acid substitution in the GFFKR sequence of the cytoplasmic domain of the integrin IIb subunit in a patient with a Glanzmann's thrombasthenia-like syndrome. *Blood.* 1998; 92(11):4178-4187.
8. Ghevaert C, Salsmann A, Watkins NA, et al. A nonsynonymous SNP in the ITGB3 gene disrupts the conserved membrane-proximal cytoplasmic salt bridge in the alphaIIbbeta3 integrin and co-segregates dominantly with abnormal proplatelet formation and macrothrombocytopenia. *Blood.* 2008;111(7): 3407-3414.
9. Gresele P, Falcinelli E, Giannini S, et al. Dominant inheritance of a novel integrin beta3 mutation associated with a hereditary macrothrombocytopenia and platelet dysfunction in two Italian families. *Haematologica.* 2009;94(5):663-669.
10. Jayo A, Conde I, Lastres P, et al. L718P mutation in the membrane-proximal cytoplasmic tail of beta3 promotes abnormal alphaIIbbeta3 clustering and lipid microdomain coalescence, and associates with a thrombasthenia-like phenotype. *Haematologica.* 2010;95(7):1158-1166.
11. Kunishima S, Hamaguchi M, Saito H. Differential expression of wild-type and mutant NMMHC-IIA polypeptides in blood cells suggests cell-specific regulation mechanisms in MYH9 disorders. *Blood.* 2008;111(6):3015-3023.
12. Kunishima S, Lopez JA, Kobayashi S, et al. Missense mutations of the glycoprotein (GP) Ibbeta gene impairing the GPIb alpha/beta disulfide linkage in a family with giant platelet disorder. *Blood.* 1997;89(7):2404-2412.
13. Kashiwagi H, Tomiyama Y, Tadokoro S, et al. A mutation in the extracellular cysteine-rich repeat region of the beta3 subunit activates integrins alphaIIbbeta3 and alphaVbeta3. *Blood.* 1999; 93(8):2559-2568.
14. Kashiwagi H, Shiraga M, Kato H, et al. Expression and subcellular localization of WAVE isoforms in the megakaryocyte/platelet lineage. *J Thromb Haemost.* 2005;3(2):361-368.
15. Sanuki S, Hamanaka S, Kaneko S, et al. A new red fluorescent protein that allows efficient marking of murine hematopoietic stem cells. *J Gene Med.* 2008;10(9):965-971.
16. Suzuki A, Obi K, Urabe T, et al. Feasibility of ex vivo gene therapy for neurological disorders using the new retroviral vector GCDNsap packaged in the vesicular stomatitis virus G protein. *J Neurochem.* 2002;82(4):953-960.
17. Ory DS, Neugeboren BA, Mulligan RC. A stable human-derived packaging cell line for production of high titer retrovirus/vesicular stomatitis virus G pseudotypes. *Proc Natl Acad Sci U S A.* 1996; 93(21):11400-11406.
18. Poncz M, Eisman R, Heidenreich R, et al. Structure of the platelet membrane glycoprotein IIb: homology to the alpha subunits of the vitronectin and fibronectin membrane receptors. *J Biol Chem.* 1987;262(18):8476-8482.

19. Kunishima S, Kobayashi R, Itoh TJ, Hamaguchi M, Saito H. Mutation of the beta1-tubulin gene associated with congenital macrothrombocytopenia affecting microtubule assembly. *Blood.* 2009;113(2):458-461.
20. Hughes PE, Diaz-Gonzalez F, Leong L, et al. Breaking the integrin hinge: a defined structural constraint regulates integrin signaling. *J Biol Chem.* 1996;271(12):6571-6574.
21. Lau TL, Kim C, Ginsberg MH, Ulmer TS. The structure of the integrin alphaIIbbeta3 transmembrane complex explains integrin transmembrane signalling. *EMBO J.* 2009;28(9): 1351-1361.
22. Schaffner-Reckinger E, Salsmann A, Debili N, et al. Overexpression of the partially activated alphaIIbbeta3D723H integrin salt bridge mutant downregulates RhoA activity and induces microtubule-dependent proplatelet-like extensions in Chinese hamster ovary cells. *J Thromb Haemost.* 2009;7(7):1207-1217.
23. Mor-Cohen R, Rosenberg N, Peretz H, et al. Disulfide bond disruption by a beta3-Cys549Arg mutation in six Jordanian families with Glanzmann thrombasthenia causes diminished production of constitutively active alphaIIbbeta3. *Thromb Haemost.* 2007;98(6):1257-1265.
24. Ruiz C, Liu CY, Sun QH, et al. A point mutation in the cysteine-rich domain of glycoprotein (GP) IIIa results in the expression of a GPIIb-IIIa (alphaIIbbeta3) integrin receptor locked in a high-affinity state and a Glanzmann thrombasthenia-like phenotype. *Blood.* 2001;98(8): 2432-2441.
25. Fuentes R, Wang Y, Hirsch J, et al. Infusion of mature megakaryocytes into mice yields functional platelets. *J Clin Invest.* 2010;120(11):3917-3922.

Rapid diagnosis of FHL3 by flow cytometric detection of intraplatelet Munc13-4 protein

Yuuki Murata,[1] Takahiro Yasumi,[1] Ryutaro Shirakawa,[2] Kazushi Izawa,[1] Hidemasa Sakai,[1] Junya Abe,[1] Naoko Tanaka,[1] Tomoki Kawai,[1] Koichi Oshima,[3-5] Megumu Saito,[3] Ryuta Nishikomori,[1] Osamu Ohara,[4,5] Eiichi Ishii,[6] Tatsutoshi Nakahata,[3] Hisanori Horiuchi,[2] and Toshio Heike[1]

[1]Department of Pediatrics, Kyoto University Graduate School of Medicine, Kyoto, Japan; [2]Department of Molecular and Cellular Biology, Institute of Development, Aging and Cancer, Tohoku University, Sendai, Japan; [3]Clinical Application Department, Center for iPS Cell Research and Application, Kyoto University, Kyoto, Japan; [4]Department of Human Genome Research, KAZUSA DNA Research Institute, Kisarazu, Japan; [5]Laboratory for Immunogenomics, Research Center for Allergy and Immunology, RIKEN, Yokohama, Japan; and [6]Department of Pediatrics, Ehime University Graduate School of Medicine, Toon, Japan

Familial hemophagocytic lymphohistiocytosis (FHL) is a potentially lethal genetic disorder of immune dysregulation that requires prompt and accurate diagnosis to initiate life-saving immunosuppressive therapy and to prepare for hematopoietic stem cell transplantation. In the present study, 85 patients with hemophagocytic lymphohistiocytosis were screened for FHL3 by Western blotting using platelets and by natural killer cell lysosomal exocytosis assay. Six of these patients were diagnosed with FHL3. In the acute disease phase requiring platelet transfusion, it was difficult to diagnose FHL3 by Western blot analysis or by lysosomal exocytosis assay. In contrast, the newly established flow cytometric analysis of intraplatelet Munc13-4 protein expression revealed bimodal populations of normal and Munc13-4–deficient platelets. These findings indicate that flow cytometric detection of intraplatelet Munc13-4 protein is a sensitive and reliable method to rapidly screen for FHL3 with a very small amount of whole blood, even in the acute phase of the disease. (*Blood.* 2011;118(5):1225-1230)

Introduction

The granule-dependent cytotoxic pathway is a major immune effector mechanism used by cytotoxic T lymphocytes (CTLs) and natural killer (NK) cells.[1] The pathway involves a series of steps, including cell activation, polarization of the lysosomal granules to the immunologic synapse, exocytosis of lytic proteins such as perforin and granzymes, and induction of apoptosis in the target cells.[2] In addition to its central role in the defense against intracellular infections and in tumor immunity, this pathway also plays an important role in the regulation of immune homeostasis. Defects in the granule-dependent cytotoxic pathway result in a catastrophic hyperinflammatory condition known as hemophagocytic lymphohistiocytosis (HLH).[1,3]

HLH is a life-threatening syndrome of immune dysregulation resulting from the uncontrolled activation and proliferation of CTLs, which leads to macrophage activation and the excessive release of inflammatory cytokines.[4,5] Clinical diagnosis of HLH is made on the basis of cardinal signs and symptoms including prolonged fever and hepatosplenomegaly, and by characteristic laboratory findings such as pancytopenia, hyperferritinemia, hypofibrinogenemia, increased levels of soluble IL-2 receptor, and low or absent NK cell activity.[5,6] HLH can be classified into primary (genetic) or secondary (acquired) forms according to the underlying etiology, although this distinction is difficult to make in clinical practice.[4,5]

Familial hemophagocytic lymphohistiocytosis (FHL) encompasses major forms of primary HLH for which mutations in the genes encoding perforin (*PRF1*; FHL2),[7] Munc13-4 (*UNC13D*; FHL3),[8] syntaxin-11 (*STX11*; FHL4),[9] and syntaxin-binding protein 2 (also known as Munc18-2) (*STXBP2*; FHL5)[10,11] have been identified to date. Perforin is a cytolytic effector that forms a pore-like structure in the target cell membrane. Munc13-4, syntaxin-11, and Munc18-2 are involved in intracellular trafficking or the fusion of cytolytic granules to the plasma membrane and the subsequent delivery of their contents into target cells.[1,12] Consequently, defective cytotoxic activity of CTLs and NK cells is one of the hallmark findings of FHL,[7,8,13-16] although NK cell activity is also decreased in some cases of secondary HLH.[15,17-20]

Prompt and accurate diagnosis of FHL is mandatory to initiate life-saving immunosuppressive therapy and to prepare for hematopoietic stem cell transplantation. Detection of perforin expression in NK cells with flow cytometry is a reliable method to screen for FHL2.[21] Another test analyzes the expression of CD107a on the surface of NK cells, which marks the release of cytolytic granules.[22] Reduced expression of CD107a implies impaired degranulation of NK cells and predicts a likelihood of FHL3.[23] However, this analysis is not available in some patients with extremely reduced NK cell numbers, such as during the acute phase of HLH.[19] In addition, NK-cell degranulation is also impaired in FHL4[24] and FHL5,[10,11] making it impossible to differentiate these disorders.

We reported previously that Munc13-4 protein is expressed in platelets and regulates the secretion of dense core granules.[25] Herein we report that Munc13-4 is expressed far more abundantly in platelets than in PBMCs. We also describe the development of a new method to screen for FHL3 rapidly by detecting intraplatelet Munc13-4 expression through flow cytometry.

Submitted January 10, 2011; accepted May 23, 2011. Prepublished online as *Blood* First Edition paper, June 8, 2011; DOI 10.1182/blood-2011-01-329540.

The online version of this article contains a data supplement.

The publication costs of this article were defrayed in part by page charge payment. Therefore, and solely to indicate this fact, this article is hereby marked "advertisement" in accordance with 18 USC section 1734.

From bloodjournal.hematologylibrary.org at MEDICAL LIBRARY OF NAGOYA UNIV on March 12, 2012. For personal use only.

Methods

Patients

Between January 2008 and March 2010, whole blood samples from 85 patients were screened for FHL3. The patients had been clinically diagnosed with HLH by their referring physicians and were suspected of possible FHL. Characteristics of the enrolled patients are summarized in supplemental Table 1 (available on the *Blood* Web site; see the Supplemental Materials link at the top of the online article). As a control, blood obtained from healthy adults at the time of patient sampling was shipped for screening along with the patient samples. Before the laboratory studies were performed, informed consent was obtained from the patients and their parents, in accordance with the institutional review board of Kyoto University Hospital and the Declaration of Helsinki.

Preparation of PBMCs and platelet samples

Whole blood samples treated with EDTA were centrifuged gently at 100*g* for 10 minutes, and platelets were collected from the supernatant plasma layer. Alternatively, platelets were prepared from small aliquots of blood samples by lysing red blood cells with ammonium chloride. PBMCs were obtained by Ficoll-Hypaque density gradient centrifugation from the remaining sample. $CD4^+$, $CD8^+$, $CD14^+$, $CD19^+$, and $CD45^+$ cells were separated from PBMCs using an AutoMACS Pro (Miltenyi Biotec) and magnetic bead–conjugated mAbs according to the manufacturer's instructions. Flow cytometric analysis revealed that each cell population contained > 95% $CD4^+$, $CD8^+$, $CD14^+$, $CD19^+$, and $CD45^+$ cells (data not shown).

Mutation analysis

Genomic DNA was isolated from the PBMCs of patients with defective Munc13-4 expression using standard procedures. Primers were designed for the amplification and direct DNA sequencing of the *UNC13D*-coding exons, including the adjacent intronic sequences for the identification of splice-site variants. Primer sequences are available upon request. Products were sequenced directly with an ABI3130 genetic analyzer (Applied Biosystems).

Antibodies

Rabbit polyclonal antibodies raised against the N-terminal region (residues 1-262)[25] and full-length human Munc13-4 protein were used as primary antibodies for Western blot and flow cytometric analysis, respectively. Rabbit polyclonal anti-integrin αIIb (Santa Cruz Biotechnology) and mouse polyclonal anti–β-actin (Sigma-Aldrich) antibodies were used as primary antibodies for Western blotting. The mAbs used in the flow cytometric analysis were FITC-conjugated anti-CD3 (SK7; BD Pharmingen), phycoerythrin (PE)–conjugated anti-CD41a (HIP8; BD Pharmingen); allophycocyanin-conjugated anti-CD56 (N901; Beckman Coulter), and PE-conjugated anti-CD107a (H4A3; eBioscience).

Western blot analysis

Cell extracts were fractionated by SDS-PAGE, and the fractionated proteins were electrotransferred onto polyvinylidene fluoride membranes. The membranes were blocked overnight in blocking buffer (5% skim milk) and incubated for 1 hour at room temperature with the primary antibodies, followed by HRP-conjugated anti–rabbit or anti–mouse IgG polyclonal antibodies (Santa Cruz Biotechnology). Specific bands were visualized by the standard enhanced chemiluminescence method.

Flow cytometric analysis of Munc13-4 protein

After surface staining with anti-CD41a mAbs, platelets were fixed and permeabilized by Cytofix/Cytoperm (BD Biosciences) and washed 3 times with Perm/Wash buffer (BD Biosciences). After nonspecific reactions were blocked with Chrome-Pure human IgG (Jackson ImmunoResearch Laboratories), rabbit polyclonal antibody against the full-length human Munc13-4 protein was added, followed by FITC-conjugated donkey anti–rabbit IgG (Jackson ImmunoResearch Laboratories). Platelets were gated on the basis of their appearance on forward- and side-scatter plots in log/log scale and by CD41a expression. The gated platelets were analyzed for Munc13-4 expression by flow cytometry (FACSCalibur; BD Biosciences).

Lysosomal degranulation assays

To quantify lysosome exocytosis by NK cells, 2×10^5 PBMCs were mixed with 2×10^5 human erythroleukemia cell line K562 cells and incubated for 2 hours in complete medium (RPMI 1640 medium supplemented with 2mM L-glutamine and 10% FCS) at 37°C in 5% CO_2. Cells were resuspended in PBS supplemented with 2% FCS and 2mM EDTA; stained with anti-CD3–FITC, anti-CD56–allophycocyanin, and anti-CD107a–PE mAbs; and analyzed by flow cytometry.

Platelet exocytosis of the lysosomal granules was analyzed as described previously[26] but with a minor modification. Briefly, platelets were suspended in PBS containing 2mM EDTA and PE-conjugated anti-CD107a mAb, stimulated with 5 U/mL of thrombin (Wako Pure Chemical Industries) for 10 minutes at 25°C, and immediately analyzed by flow cytometry. The degranulation index of platelets was calculated as: (mean fluorescence value of stimulated sample − mean fluorescence value of nonstimulated sample)/mean fluorescence value of nonstimulated sample.

Statistical analysis

Statistical analyses were performed with 1-way ANOVA followed by the Tukey post hoc test to compare multiple groups, with a $P < .05$ level considered to be significant.

Results

Diagnosis of FHL3 by Western blot analysis using platelets

Before screening for FHL3, the Munc13-4 expression level was compared between platelets and PBMCs. Munc13-4 expression in platelets was approximately 10 times higher than that in PBMCs (Figure 1A). $CD8^+$ cells expressed a similar level of Munc13-4 protein as other PBMC cell types (Figure 1B). Similar amounts of platelet- and PBMC-derived proteins could be obtained from a sample (data not shown). Therefore, platelets were used to perform Western blotting to screen for Munc13-4 deficiency. Of the 85 patients screened, 6 patients were diagnosed with FHL3 (Figure 1C). Munc13-4 protein was barely detected in the platelets of each FHL3 patient regardless of the gene mutation (Table 1). For each sample, no more than 1 mL of whole blood was required to perform the analysis.

Difficulty in diagnosing FHL3 in the acute phase of the disease

Patients in the acute phase of the disease who require screening for FHL often receive platelet transfusions because of thrombocytopenia.[4-6] To study the effect of transfused platelets on screening results, FHL3 screening was attempted in a patient receiving platelet transfusions. As expected, Western blotting using platelets could not detect Munc13-4 deficiency because of the normal expression of the protein in the transfused platelets (Figure 2A left column). Surprisingly, Western blotting using PBMCs also could not clearly identify Munc13-4 deficiency because a substantial number of platelets were present in the PBMCs obtained by the standard method (Figure 2A right column). By positively selecting $CD45^+$ cells and removing platelets, it was found that a considerable amount of the Munc13-4 protein detected in PBMC samples

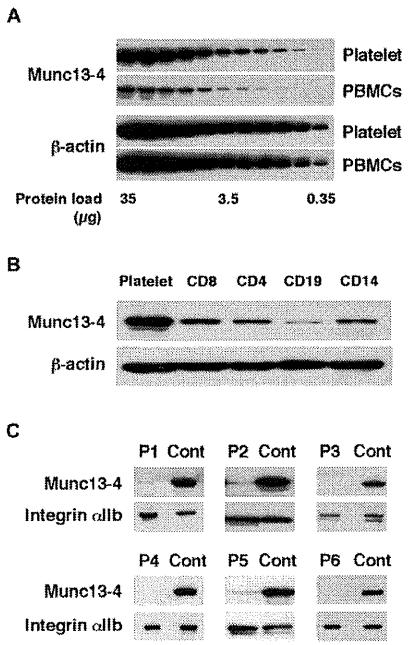

Figure 1. Diagnosing FHL3 by Western blotting using platelet protein. The amount of Munc13-4 protein expression was compared between platelets and PBMCs (A) and among platelets, $CD8^+$, $CD4^+$, $CD19^+$, and $CD14^+$ cells (B) by Western blotting. A representative result of 5 independent experiments is shown. (C) Six FHL3 patients were diagnosed by Western blotting for Munc13-4 protein using platelets.

obtained by standard density gradient centrifugation was actually derived from the contaminating platelets (Figure 2B).

We performed a NK-cell degranulation assay for every referred sample and found the assay to be defective for every FHL3 patient identified (data not shown). All of the other patients showed a normal release of lysosomal granules by NK cells; however, the analysis could not be performed in some patients because of the extremely low NK-cell number during the acute phase of the disease (data not shown).

We also examined the lysosomal granule release of platelets in 31 patients to determine whether this assay could be used as a screening method for FHL3. Lysosomal exocytosis of FHL3 platelets was partially impaired at steady state, but profound impairment was observed during the acute phase of the disease (Figure 3A-C). This profound impairment was also observed in platelets obtained from some secondary HLH patients during the acute phase (Figure 3B-C). These results indicate that it is difficult to diagnose FHL3 during the acute phase of HLH either by Western blot or by lysosomal degranulation assay.

Table 1. UNC13D gene mutations of FHL3 patients

Patient	Age at onset	Gender	Mutation	Genotype	Predicted effect
P1	14 days	Female	c.1596 + 1G → C	Homo	Splice error
P2	2 months	Male	c.322–1G → A	Hetero	Splice error
			c.990G → C	Hetero	p.Q330H
			c.3193C → T	Hetero	p.R1065X
P3	12 months	Female	c.754–1G → C	Hetero	Splice error
			c.2485delC	Hetero	p.L829fs
P4	4 months	Female	c.754–1G → C	Hetero	Splice error
			c.1799C → T	Hetero	p.T600M
			c.1803C → A	Hetero	p.Y601X
P5	2 months	Female	c.754–1G → C	Hetero	Splice error
			c.1596 + 1G → C	Hetero	Splice error
P6	5 months	Male	ND	ND	ND

Mutations were checked for single nucleotide polymorphisms using the dbSNP Build 132 database from the National Center for Biotechnology Information.

X indicates stop; fs, frame shift; and ND, not determined.

Rapid diagnosis of FHL3 by flow cytometric detection of intraplatelet Munc13-4

To overcome the difficulty in diagnosing FHL3 during the acute phase of HLH, antibodies were raised against the full-length human Munc13-4 protein (supplemental Figure 1) and a new method was developed to detect Munc13-4 protein in platelets by flow cytometry. A total of 35 patients, including 4 with FHL3 (P3-P6), were

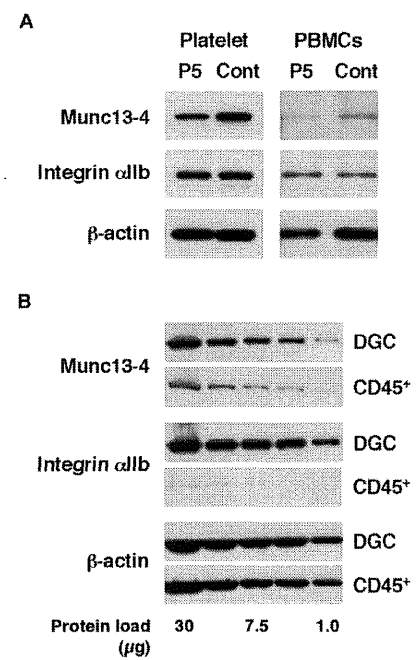

Figure 2. Effect of platelet transfusion on Western blot analysis. (A) Western blotting analysis for Munc13-4 expression using platelets and PBMCs from an FHL3 patient (P5) receiving platelet transfusions during the acute phase of the disease. (B) The expression of Munc13-4 was compared between PBMCs obtained by density gradient centrifugation (DGC) and $CD45^+$ cells obtained by magnetic sorting from healthy controls. A representative result of 3 independent experiments is shown.

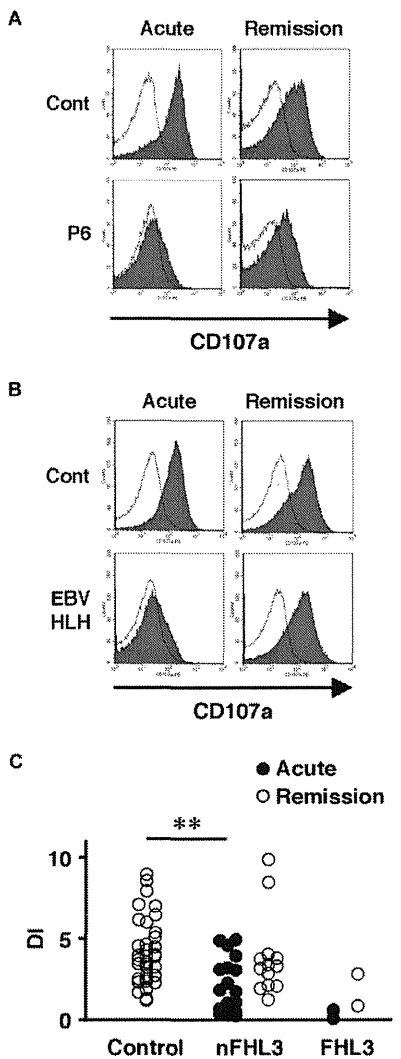

Figure 3. Analysis of lysosomal exocytosis using platelets from HLH patients. Platelets from an FHL3 patient (P6; A) and from a secondary (EBV-associated) HLH patient (B) along with healthy controls were left untreated (open histogram) or were stimulated with thrombin (closed histograms), and the surface expression of CD107a was analyzed by flow cytometry. Analysis was performed during the acute phase of the disease (left column) and after clinical remission (right column). (C) Degranulation index (DI) of platelets from HLH patients during the acute phase (●) and after clinical remission (○). HLH patients with normal NK-cell degranulation and Munc13-4 protein expression by Western blot analysis were defined as non-FHL3 (nFHL3). $^{**}P < .01$ by the Tukey post hoc test.

analyzed using this method. Munc13-4 deficiency was readily detected in all of the FHL3 patients, with a sample volume of < 100 μL of whole blood (Figure 4A-C). Munc13-4 protein was expressed at normal level in the platelets of parents and siblings of FHL3 patients carrying heterozygous *UNC13D* mutations (data not shown). In the FHL3 patient receiving platelet transfusions, flow cytometric analysis revealed bimodal populations of normal and Munc13-4–deficient platelets (P5 in Figure 4A). As shown in Figure 4B, the method was able to clearly identify Munc13-4–deficient platelets in whole blood samples stored at room temperature for 1 week.

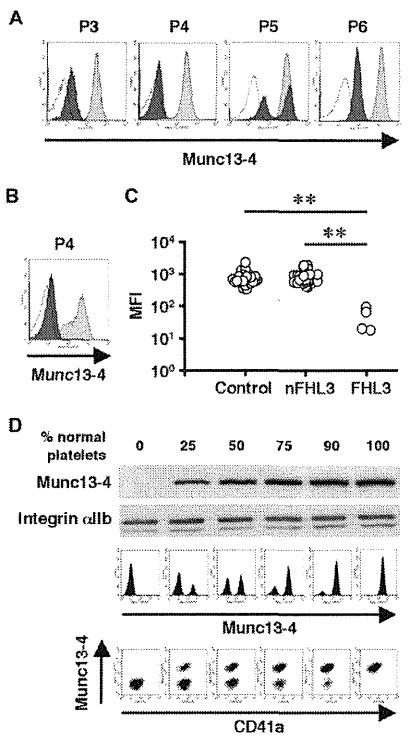

Figure 4. Flow cytometric detection of intraplatelet Munc13-4 protein. Flow cytometric analysis of intraplatelet Munc13-4 expression in 4 FHL3 patients and healthy controls using whole blood samples shipped overnight (A) and in an FHL3 patient (P4) and a healthy control using samples stored at room temperature for a week (B). Dark closed histograms represent platelets from FHL3 patients, whereas light closed histograms represent platelets from healthy controls. Open histograms represent staining with isotype controls. (C) Mean fluorescence intensity (MFI) of intraplatelet Munc13-4 staining for HLH patients and healthy controls. All of the healthy controls (n = 35) were adults. Non-FHL3 (nFHL3) patients (n = 31), as defined in Figure 3, varied in age (2 days-39 years) and included 2 patients with FHL2. Age-related variations in the MFI of Munc13-4 staining were not observed. $^{**}P < .01$ by the Tukey post hoc test. (D) The sensitivities of Western blot and flow cytometric analyses for detecting Munc13-4–deficient platelets were compared.

To determine the sensitivity of the new method, Munc13-4–deficient platelets were mixed with normal platelets at varying ratios. Western blot analysis could not detect Munc13-4–deficient platelets easily, even when the proportion of normal platelets was as low as 25% (Figure 4D). In contrast, flow cytometric analysis easily identified 10% Munc13-4–deficient platelets among 90% normal platelets (Figure 4D), which proved the high sensitivity of the method in diagnosing FHL3.

Discussion

FHL is a rare but life-threatening inherited immune disorder for which mutations in 4 genes have been identified as causative factors. *PRF1* encodes the cytolytic effector protein perforin that forms a pore-like structure in the target cell membrane.[1,12] A mutation in *PRF1* results in FHL2,[7] which accounts for 20%-50% of FHL cases.[4,5] *UNC13D* encodes the protein Munc13-4, which is crucial for the fusion of cytolytic granules to the plasma membrane and the subsequent release of perforin and granzymes.[1,12] Mutations in *UNC13D* result in FHL3,[8] which accounts for 20%-30% of FHL cases.[4,12] FHL4 is caused by mutations in *STX11*, which encodes syntaxin-11.[9] Mutations in *STXBP2*, which encodes Munc18-2, were recently reported to cause FHL5.[10,11] Syntaxin-11 and Munc18-2 also mediate the fusion of cytolytic granules to the plasma membrane.[1,5,12] The ability to screen for FHL2-5 rapidly would facilitate the initiation of life-saving immunosuppressive therapy and the preparation of FHL patients for hematopoietic stem cell transplantation.

In the present study, we found that the Munc13-4 protein is expressed abundantly in platelets (Figure 1A-B). The detection of Munc13-4 protein in platelets by Western blotting (Figure 1C) or flow cytometry (Figure 4A-B) was a reliable screening method to identify FHL3 patients. Munc13-4–deficient platelets were identified easily among normal transfused platelets by flow cytometry, which indicated that this method could be applied to patients who are receiving platelet transfusions during the acute phase of the disease (P5 in Figure 4A). Detection of intraplatelet Munc13-4 was enabled by the use of highly specific antibodies against the full-length human Munc13-4 (supplemental Figure 1).

There is a possibility that FHL3 patients with residual Munc13-4 protein expression could be overlooked by the screening methods described in this study. Most FHL3 patients have mutations that result in the absence or significant reduction of Munc13-4 protein expression,[16,23] as was the case with the patients screened in this study (Figure 1C), which suggests that the mutated Munc13-4 protein is unstable. The NK-cell degranulation assay, which was performed for every referred sample with a sufficient number of NK cells, revealed defective degranulation only in the identified FHL3 patients (date not shown). These results indicate that the majority of mutations in *UNC13D* are likely amenable to rapid detection by the new methods described in this study. Comparative studies on the *UNC13D* genotype, Munc13-4 protein expression, and the lysosomal exocytosis assay must be performed to confirm the reliability of these methods.

It was also investigated whether the analysis of lysosomal release by platelets could be used as an alternative method to screen for FHL3. Profound impairment of lysosomal exocytosis by platelets during the acute phase of the disease and restoration of this impairment after clinical remission was observed in FHL3 and in some secondary HLH patients (Figure 3). It is not clear whether this transient impairment of platelet degranulation is involved in HLH pathogenesis or if it merely reflects in vivo platelet activation by diffuse endothelial damage during the acute phase of the disease that renders them unresponsive to ex vivo stimulation. The release of lysosomal granules by Munc13-4–deficient platelets was impaired only minimally at steady state (Figure 3A and 3C), which is in contrast to a recent study showing the involvement of the Munc13-4 protein in the release of lysosomal granules in mouse platelets.[27] Although the precise reason for this discrepancy is unclear, platelet degranulation is likely to be regulated differentially between species; for example, Munc13-4–deficient mice have bruising and bleeding tendencies[27] that are not commonly associated with human FHL3. Further studies are warranted to elucidate the exocytosis pathways of platelets and their role in the pathophysiology of HLH.

With the development of tools for rapid screening, the diagnostic approach for FHL has changed over the years. Impaired NK cytotoxicity was the first reported signature clinical finding of FHL patients.[13,14] Defective CTL activity was subsequently reported as another hallmark of FHL.[7,8,16,28] However, NK-cell activity is also decreased in some cases of secondary HLH,[15,17-20] and the CTL cytotoxicity assay is not readily accessible to most clinicians. The NK-cell lysosomal exocytosis assay is a comprehensive method to identify patients with a degranulation defect.[10,11,22-24] However, this analysis is not available in some patients with extremely reduced NK-cell numbers, which are often observed during the acute phase of HLH.[19] Although CTLs can be an alternative tool to perform the lysosomal exocytosis assay,[24,28,29] it remains impossible to differentiate FHL3-FHL5.[10,11,23,24] Impairment in these assays warrants the genetic confirmation of FHL, but sequencing all of the candidate genes is not a suitable approach for rapid diagnosis. Flow cytometric detection of perforin expression in NK cells is a reliable and rapid way of identifying patients with FHL2,[21] and the new method described in this study for the detection of Munc13-4 expression in platelets would add to the rapid diagnosis of FHL3.

Platelets could also be used for the screening of FHL4 and FHL5 because they share some granule-transport mechanisms with other types of hematopoietic cells, including CTLs and NK cells.[2,30,31] Indeed, in the present study, both syntaxin-11 and Munc18-2 were expressed abundantly in platelets (data not shown). We are currently using platelet proteins to screen for FHL4-FHL5 by Western blot analysis, although no cases have been found so far because of the extreme rarity of these disorders.

In summary, platelets abundantly express Munc13-4 protein and are a useful tool to screen for FHL3. By detecting intraplatelet Munc13-4 expression by flow cytometry, it is now possible to rapidly screen for FHL3 with a very small sample of whole blood, even in the acute disease phase requiring platelet transfusion. Because platelets share some of their granule transport systems with other types of hematopoietic cells, they could also be used to screen for other types of immune disorders, including FHL4 and FHL5.

Acknowledgments

The authors are grateful to all of the participating patients, their families, and the referring physicians for their generous cooperation in this study.

This study was supported by grants from The Morinaga Foundation for Health and Nutrition; from the Japanese Ministry of Education, Culture, Sports, Science, and Technology; and from the Japanese Ministry of Health, Labor, and Welfare.

Authorship

Contribution: T.Y., R.N., T.N., H.H., and H.T. designed the research; Y.M., K.I., and M.S. performed the Western blot and flow cytometric analyses; K.O. and O.O. performed the genetic analyses; R.S. and H.H. prepared the anti–Munc13-4 antibodies and started the FHL3 screening; Y.M., T.Y., R.S., K.I., H.S., J.A., N.T., T.K., R.N., E.I., T.N., H.H., and T.H. analyzed and discussed the results; and Y.M., T.Y., and T.H. wrote the manuscript.

Conflict-of-interest disclosure: The authors declare no competing financial interests.

Correspondence: Takahiro Yasumi, Department of Pediatrics, Kyoto University Graduate School of Medicine, 54 Kawahara-cho, Shogoin, Sakyo-ku, Kyoto, 606-8507 Japan; e-mail: yasumi@kuhp.kyoto-u.ac.jp or Hisanori Horiuchi, Department of Molecular and Cellular Biology, Institute of Development, Aging and Cancer, Tohoku University, 4-1 Seiryo-machi, Aoba-ku, Sendai 980-8575 Japan; e-mail: horiuchi@idac.tohoku.ac.jp.

References

1. Fischer A, Latour S, de Saint Basile G. Genetic defects affecting lymphocyte cytotoxicity. *Curr Opin Immunol.* 2007;19(3):348-353.
2. Hong W. Cytotoxic T lymphocyte exocytosis: bring on the SNAREs! *Trends Cell Biol.* 2005; 15(12):644-650.
3. Ménasché G, Feldmann J, Fischer A, de Saint Basile G. Primary hemophagocytic syndromes point to a direct link between lymphocyte cytotoxicity and homeostasis. *Immunol Rev.* 2005;203: 165-179.
4. Janka GE. Familial and acquired hemophagocytic lymphohistiocytosis. *Eur J Pediatr.* 2007; 166(2):95-109.
5. Gupta S, Weitzman S. Primary and secondary hemophagocytic lymphohistiocytosis: clinical features, pathogenesis and therapy. *Expert Rev Clin Immunol.* 2010;6(1):137-154.
6. Créput C, Galicier L, Buyse S, Azoulay E. Understanding organ dysfunction in hemophagocytic lymphohistiocytosis. *Intensive Care Med.* 2008; 34(7):1177-1187.
7. Stepp S, Dufourcq-Lagelouse R, Le Deist F, et al. Perforin gene defects in familial hemophagocytic lymphohistiocytosis. *Science.* 1999;286(5446): 1957-1959.
8. Feldmann J, Callebaut I, Raposo G, et al. Munc13-4 is essential for cytolytic granules fusion and is mutated in a form of familial hemophagocytic lymphohistiocytosis (FHL3). *Cell.* 2003; 115(4):461-473.
9. zur Stadt U, Schmidt S, Kasper B, et al. Linkage of familial hemophagocytic lymphohistiocytosis (FHL) type-4 to chromosome 6q24 and identification of mutations in syntaxin 11. *Hum Mol Genet.* 2005;14(6):827-834.
10. zur Stadt U, Rohr J, Seifert W, et al. Familial hemophagocytic lymphohistiocytosis type 5 (FHL-5) is caused by mutations in Munc18-2 and impaired binding to syntaxin 11. *Am J Hum Genet.* 2009; 85(4):482-492.
11. Côte M, Ménager M, Burgess A, et al. Munc18-2 deficiency causes familial hemophagocytic lymphohistiocytosis type 5 and impairs cytotoxic granule exocytosis in patient NK cells. *J Clin Invest.* 2009;119(12):3765-3773.
12. Cetica V, Pende D, Griffiths GM, Aricò M. Molecular basis of familial hemophagocytic lymphohistiocytosis. *Haematologica.* 2010;95(4):538-541.
13. Perez N, Virelizier JL, Arenzana-Seisdedos F, Fischer A, Griscelli C. Impaired natural killer activity in lymphohistiocytosis syndrome. *J Pediatr.* 1984;104(4):569-573.
14. Aricò M, Nespoli L, Maccario R, et al. Natural cytotoxicity impairment in familial haemophagocytic lymphohistiocytosis. *Arch Dis Child.* 1988;63(3): 292-296.
15. Schneider EM, Lorenz I, Müller-Rosenberger M, Steinbach G, Kron M, Janka-Schaub GE. Hemophagocytic lymphohistiocytosis is associated with deficiencies of cellular cytolysis but normal expression of transcripts relevant to killer-cell-induced apoptosis. *Blood.* 2002;100(8): 2891-2898.
16. Ishii E, Ueda I, Shirakawa R, et al. Genetic subtypes of familial hemophagocytic lymphohistiocytosis: correlations with clinical features and cytotoxic T lymphocyte/natural killer cell functions. *Blood.* 2005;105(9):3442-3448.
17. Schneider EM, Lorenz I, Walther P, Janka-Schaub GE. Natural killer deficiency: a minor or major factor in the manifestation of hemophagocytic lymphohistiocytosis? *J Pediatr Hematol Oncol.* 2003;25(9):680-683.
18. Grom AA, Villanueva J, Lee S, Goldmuntz EA, Passo MH, Filipovich A. Natural killer cell dysfunction in patients with systemic-onset juvenile rheumatoid arthritis and macrophage activation syndrome. *J Pediatr.* 2003;142(3):292-296.
19. Grom AA. Natural killer cell dysfunction: A common pathway in systemic-onset juvenile rheumatoid arthritis, macrophage activation syndrome, and hemophagocytic lymphohistiocytosis? *Arthritis Rheum.* 2004;50(3):689-698.
20. Horne A, Zheng C, Lorenz I, et al. Subtyping of natural killer cell cytotoxicity deficiencies in haemophagocytic lymphohistiocytosis provides therapeutic guidance. *Br J Haematol.* 2005;129(5): 658-666.
21. Kogawa K, Lee SM, Villanueva J, Marmer D, Sumegi J, Filipovich AH. Perforin expression in cytotoxic lymphocytes from patients with hemophagocytic lymphohistiocytosis and their family members. *Blood.* 2002;99(1):61-66.
22. Alter G, Malenfant JM, Altfeld M. CD107a as a functional marker for the identification of natural killer cell activity. *J Immunol Methods.* 2004; 294(1-2):15-22.
23. Marcenaro S, Gallo F, Martini S, et al. Analysis of natural killer-cell function in familial hemophagocytic lymphohistiocytosis (FHL): defective CD107a surface expression heralds Munc13-4 defect and discriminates between genetic subtypes of the disease. *Blood.* 2006;108(7): 2316-2323.
24. Bryceson YT, Rudd E, Zheng C, et al. Defective cytotoxic lymphocyte degranulation in syntaxin-11 deficient familial hemophagocytic lymphohistiocytosis 4 (FHL4) patients. *Blood.* 2007;110(6): 1906-1915.
25. Shirakawa R, Higashi T, Tabuchi A, et al. Munc13-4 is a GTP-Rab27-binding protein regulating dense core granule secretion in platelets. *J Biol Chem.* 2004;279(11):10730-10737.
26. Febbraio M, Silverstein RL. Identification and characterization of LAMP-1 as an activation-dependent platelet surface glycoprotein. *J Biol Chem.* 1990;265(30):18531-18537.
27. Ren Q, Wimmer C, Chicka MC, et al. Munc13-4 is a limiting factor in the pathway required for platelet granule release and hemostasis. *Blood.* 2010; 116(6):869-877.
28. Nagai K, Yamamoto K, Fujiwara H, et al. Subtypes of familial hemophagocytic lymphohistiocytosis in Japan based on genetic and functional analyses of cytotoxic T lymphocytes. *PLoS ONE.* 2010;5(11):e14173.
29. Rohr J, Beutel K, Maul-Pavicic A, et al. Atypical familial hemophagocytic lymphohistiocytosis due to mutations in UNC13D and STXBP2 overlaps with primary immunodeficiency diseases. *Haematologica.* 2010;95(12):2080-2087.
30. Stinchcombe J, Bossi G, Griffiths G. Linking albinism and immunity: the secrets of secretory lysosomes. *Science.* 2004;305(5680):55-59.
31. Ren Q, Ye S, Whiteheart SW. The platelet release reaction: just when you thought platelet secretion was simple. *Curr Opin Hematol.* 2008;15(5): 537-541.